İSTANBUL TECHNICAL UNIVERSITY ★ INSTITUTE OF SCIENCE AND TECHNOLOGY

ENERGY HARVESTING FROM PASSIVE HUMAN MOTION

M.Sc. Thesis by
Fatih GÜRDAL

Department : Electrical Engineering

Programme : Electrical Engineering

Thesis Supervisor: Asst. Prof. Dr. Deniz YILDIRIM

JULY 2010

İSTANBUL TECHNICAL UNIVERSITY ★ INSTITUTE OF SCIENCE AND TECHNOLOGY

ENERGY HARVESTING FROM PASSIVE HUMAN MOTION

M.Sc. Thesis by
Fatih GÜRDAL
(504061030)

Date of submission : **7 May 2010**
Date of defence examination: **7 June 2010**

Supervisor (Chairman) : **Asst. Prof. Dr. Deniz YILDIRIM (ITU)**
Members of the Examining Committee : **Prof. Dr. Metin GÖKAŞAN (ITU)**
Asst. Prof. Dr. Güven KÖMÜRGÖZ (ITU)

JULY 2010

İSTANBUL TEKNİK ÜNİVERSİTESİ ★ FEN BİLİMLERİ ENSTİTÜSÜ

PASİF İNSAN HAREKETİNDEN ENERJİ KAZANIMI

YÜKSEK LİSANS TEZİ
Fatih GÜRDAL
(504061030)

Tezin Enstitüye Verildiği Tarih : 7 Mayıs 2010
Tezin Savunulduğu Tarih : 7 Haziran 2010

Tez Danışmanı : Yrd. Doç. Dr. Deniz YILDIRIM (ITU)
Diğer Jüri Üyeleri: Prof. Dr. Metin GÖKAŞAN (ITU)
Yrd. Doç. Dr. Güven KÖMÜRGÖZ (ITU)

TEMMUZ 2010

FOREWORD

I would like to express my sincerest thanks to my mother and brother for their guidance, support and to my supervisor Asst. Prof. Dr. Deniz Yıldırım for his contribution throughout the preparations for this thesis.

June 2010

Fatih Gürdal
Electrical & Electronics Engineer

TABLE OF CONTENTS

Page

ABBREVIATIONS ..... **ix**
LIST OF TABLES ..... **xi**
LIST OF FIGURES ..... **xiii**
SUMMARY ..... **xv**
ÖZET ..... **xvii**
1. INTRODUCTION **1**
1.1 Need For Energy Harvesting 3
1.2 Human Is An Energy Source 5
1.2.1 Body Heat 6
1.2.2 Breath 7
1.2.3 Blood Pressure 9
1.2.4 Walking 9
2. WALKING AS AN ENERGY SOURCE **13**
2.1 Energy Harvesting- Making Use of Vertical Foot Strike Motion 13
2.2 Energy Harvesting- Making Use of Horizontal Leg Motion 18
2.2.1 Foot Motion Sliding Generator 18
3. NOVEL ENERGY HARVESTING GENERATORS BASED ON HORIZONTAL LEG MOTION **21**
3.1 Rotor and Stator Placed On Different Legs 21
3.2 Integrated Rotor and Stator with Iron Rotor Core 23
4. CONCLUSIONS **35**
4.1 Future Work 36
REFERENCES **37**
APPENDICES **39**
CURRICULUM VITA **45**

ABBREVIATIONS

ITU	: International Telecommunication Union
GPS	: Global Positioning System
3G&4G	: 3rd generation& 4th generation
PZT	: Polyleadzirconate titanate
PVDF	: Polyvinylidene fluoride
FEM	: Finite elements method
EMF	: Electromotive force

LIST OF TABLES

Page

Table 1.1: Human body activities vs. power requirements [1] 5
Table 1.2: Power consumption of some portable electronics [8] 6
Table 2.1: Characteristics of *PVDF*&*PZT* [7] 14
Table 3.1: Winding flux and rotor magnetization force distribution over rotor positions for one pole 29
Table 3.2: Movement characteristics of the rotor and stator 33
Table A.1 : Coefficients of Friction Values For Some Surfaces 40
Table A.2 : Movement and Magnetization Characteristics of The Integrated Type Designed Generator 41

LIST OF FIGURES

Page

Figure 1.1 : Energy harvesting backpack [5] 2
Figure 1.2 : Foot motion sliding generator [6] 3
Figure 1.3 : Mobile phone subscribers per 100 inhabitants 1997-2007 [1] 4
Figure 1.4 : Improvements in mobile computing technology from 1990-2003 [1] 5
Figure 1.5 : Tight band fastened around chest [10] 8
Figure 1.6 : Tight band fastened around chest on user [10] 8
Figure 2.1 : Piezoelectric material sheet 13
Figure 2.2 : *PVDF* shaped into elongated hexagon 17
Figure 2.3 : *PVDF*& *PZT* used designs energizing RF transmitter [1] 18
Figure 2.4 : Foot motion sliding generator 19
Figure 2.5 : Open circuit voltage of Foot Motion Sliding Generator 19
Figure 3.1: Separated Rotor and Stator Generator Design 22
Figure 3.2: Dimensions of the built prototype 22
Figure 3.3: Induced *emf* waveform for the generator in Figure 3.2, 500 *mV/div*-20 *ms/div* 23
Figure 3.4: Integrated type linear generator design 24
Figure 3.5: Free body diagram of rotor 24
Figure 3.6: Circular dependency between rotor position and magnetization forces. 26
Figure 3.7: Mesh drawing for FEM analysis 27
Figure 3.8: Generator magnetic field distribution for some rotor position (a) X_r=0, (b) X_r=0.25 cm, (c) X_r=0.5 cm, (d) X_r=0.75 cm, ... 28
Figure 3.9: Flux and magnetization forces vs. rotor position 30
Figure 3.10: Feasibility checking process of designed generator 31
Figure 3.11: Induced *emf* vs. time 33

ENERGY HARVESTING FROM PASSIVE HUMAN MOTION

SUMMARY

For the last two decades in the basis of the development of integrated circuit elements, the variety of electronics used in all areas of life is continuing to increase. The use of portable electronics has grown up from individual usage to biomedical and military based applications. Moreover, the dependency of the end users to these electronics is increasing parallel to the developments in information technologies.

Furthermore, with the growth of integrated circuit design technology, size and weight of portable electronics have been decreasing as well. However, the weight and size of batteries used in portable electronics are the main factors of limitations for becoming smaller of these devices. The main reason for this limitation is being much slower growth in battery technology than the other technologies employed in these electronics. However, the main problem in the use of portable electronics is the limited charge capacity of batteries.

Investigating human body motions one employs high power levels to do these motions. Therefore, researchers have suggested harvesting human energy as an alternative or auxiliary way for batteries used in portable electronics.

In this thesis it is examined some of the possible motion types which are benefited for energy harvesting. It is evaluated the parameters affecting the suitability of the motion that is used for energy harvesting. These parameters can be classified in two parts. First, it should be harvested enough power to charge battery of electronics used. Second, the physiological effects of the energy-harvesting instrument on human body should not create much stress on user. Based on these criterions, it is decided that walking is the most suitable motion type for energy harvesting.

Next, motion of walking is divided into two parts as vertical and horizontal leg motions in terms of the ways of energy harvesting. Being vertical foot motions, bending of sole and heel strike are the most popular types of motions for energy harvesting. In literature, there are many studies about energy harvesting from these motions by inserting piezoelectric materials at the sole of a shoe.

After, it is mentioned about three energy harvesting generator designs based on the horizontal motion of legs. The first one of these energy harvesting generators is based on to produce electrical energy by the principle of relative movement of its rotor to stator with placing it near the shoe of user, which is a literature study. In this linear generator design a nonmagnetic material used for the rotor body to sustain rotor easily move inside the stator. After that, it is suggested two novel energy harvesting generators based on the horizontal movement of legs. Firstly, it is proposed an energy harvesting generator of which rotor and stator are seperated from each other and placed interior sides of legs of user. Second suggestion is a linear generator design with stator and rotor placed together near the shoe of user. However, as distinct from simulants made in literature it uses a magnetic rotor core to increase the induced *emf*.

Finally, some analyses are performed based on the finite elements method to show the feasibility of the novel proposed linear generator in terms of its dimensions and properties.

PASİF İNSAN HAREKETİNDEN ENERJİ KAZANIMI

ÖZET

Son yirmi yıldır tümleşik devre elemanları teknolojisindeki gelişmeler temelinde hayatın her alanında hizmete sunulan elektronik aletlerin çeşitliliği artarak devam etmektedir. Taşınabilir elektronik aletlerinin kullanımı bireysel kullanımdan, biyomedikal ve askeri amaçlı uygulamalara kadar yaygınlaşmıştır. Buna ileve olarak son kullanıcıların bu cihazlara olan bağımlılığı bilgi teknolojilerindeki gelişmeler paralelinde artmaktadır.

Ayrıca tümleşik devre tasarım teknolojisinin gelişimiyle beraber taşınabilir elektronik aletlerinin ağırlıkları ve hacimleri de küçülmektedir. Fakat bu cihazlarda güç kaynağı olarak kullanılan pillerin ağırlıkları ve hacimleri bu küçülmeyi sınırlayan en büyük etmenlerdir. Bunun en büyük sebebi ise pil teknolojisindeki ilerlemenin bu cihazlarda kullanılan diğer teknolojilere göre oldukça yavaş ilerlemesidir. Fakat bu cihazların kullanımda oluşan en büyük problem cihazlardaki mevcut güç kaynaklarının tükenebilir olmasıdır.

İnsanın vücüt hareketleri incelendiğinde bu hareketleri yapmak için kullanılan güç miktarlarının oldukça fazla olduğu görülür. Bundan dolayı araştırmacılar taşınabilir elektroniklerde kullanılan pillere alternatif ya da yardımcı olarak insan hareketinden enerji kazanımı yöntemini öne sürmüşlerdir.

Bu tezde enerji kazanımı yapılabilecek hareket tiplerinden bazıları incelenmiştir. İncelemelerde bazı parametreler göz önüne alınarak hareketin enerji kazanımı için uygunluğu tartışılmıştır. Bu parametreler iki başlık altında sıralanabilir. Birinci olarak kullanılacak elektronik aleti şarj edebilecek miktarda enerji kazanımı sağlanılmalıdır. İkincisi, enerji kazanım aletinin kişide oluşturduğu fizyolojik etkisi kişiyi rahatsız edecek düzeyde olmamalıdır. Bu ölçüler ele alındığında enerji kazanımına en uygun hareket tipinin yürüme olduğu saptanmıştır.

Bundan sonra yürüme hareketi enerji kazanımı açısından dikey ve yatay bacak hareketi olarak iki bölümde incelenmiştir. Dikey ayak hareketi olan ayak içi kıvrılması ve topuk vuruşu hareketleri enerji kazanımı için en popüler hareket çeşitleridir. Piezo elektrik maddelerini ayakkabı altına koyarak bu hareket tiplerinden enerji kazanımı ile ilgili literatürde çok çalışmalar mevcuttur.

Daha sonra bacağın yatay hareketine bağlı olarak yapılabilecek üç farklı enerji kazanımı tasarımından söz edilmiştir. Birincisi bir enerji kazanım jeneratörünün ayak kenarına monte edilerek rotor ve statorun birbirine göre hareketi neticesinde elektrik enerjisi üretmesi prenbine dayalı bir literatür çalışmasıdır. Bu tümleşik yapılı jeneratör tasarımında rotor gövdesi olarak kullanılan manyetik olmayan malzeme rotorun stator içerisinde kolayca hareket etmesini sağlar. Bundan başka yatay ayak hareketine bağlı olarak enerji kazanımı sağlayan iki yeni jenerator tasarımı önerilmiştir. Birincisi, rotor ve statorun ayrılıp iki bacağın iç yüzeylerine koyularak yapılan bir dizayndır. İkincisi rotor ve statorun birlikte ayak kenarına yerleştirildiği bir lineer jeneratör tasarımıdır. Fakat literatürdeki benzerlerinden farklı olarak

endüklenen gerilimi artırmak amacıyla mıknatıslanma özelliği olan rotor çatısı kullanılmıştır.

Son olarak da, sonlu elemanlar yönteminden faydalanarak önerilen yeni lineer jeneratorun boyutları ve özellikleri açısından uygulanabilirliğini gösteren analizler yapılmıştır.

1. INTRODUCTION

This thesis is about energy harvesting from potential human motions. People have become more and more dependent on portable electronic devices. Today in all of the areas of daily life it is used some kind of portable electronic devices. These devices range from biomedical devices such as pacemakers, electromechanical or neuroelectric prostheses to consumer products such as cellular phones, laptops, global positioning devices. In recent years, technological developments in portable electronics have increased very fast. However as its name “portable” implies the energy source of these devices are independent which results in limited time of operation.

In recent years, it has been studying on the techniques of energy harvesting from human. Examining the motions of a human being or the physiological events happening in his body, considerable amount of energy comes out. If a little amount of this energy is scavenged, it can be used to energize a portable electronic device.

Since foot and leg exhibit large range of motion horizontally and they apply large vertical forces to ground [1] walking is a good candidate for energy harvesting. Therefore, studies held about energy harvesting from human motions focus on the motion of walking. In fact, bending of foot, heel strike and swinging of legs are the motion types held during walking.

After deciding the motion type from which the energy to be harvested it is time to design a method of energy conversion. For capturing energy from heel strike or bending of foot, several methods are proposed and studied in literature. First one, a popular way, it is benefited from piezoelectric material placed in sole of shoes. Piezoelectricity is the ability of some materials (notably crystals and certain ceramics, including bone) to generate an electric field or electric potential in response to applied mechanical stress [2]. If the material is not short-circuited, the applied stress induces a voltage across the material. In other words, piezoelectric material acts as capacitor when mechanically stressed. This effect for piezoelectric material is also reversible. That is when an electric field is applied contraction, strain

or bending happens among piezoelectric material. This material has very wide usage in industry from high voltage and power source applications such as cigarette litters, ac voltage multipliers to sensors such as ultrasonic transducers for medical imaging, sonar wave detection in submarines and actuators such as loudspeakers, atomic force microscopes and diesel engine fuel injectors. An attractive study made [3] where piezoelectric sheets used for recovering energy from ocean waves.

In literature in addition to piezoelectric materials, there are several practices using electromagnetic generators for harvesting energy from walking. In one of these practices, principle of regenerative braking is benefited for capturing energy [4]. In that study, 0.8 *watts* power recovered from the negative work done at the time interval of knee bending. Besides, an attractive design made where an energy harvesting backpack mechanism used for energy harvesting. In the proposed design, the backpack load is suspended via springs from the backpack frame as shown in Figure 1.1.

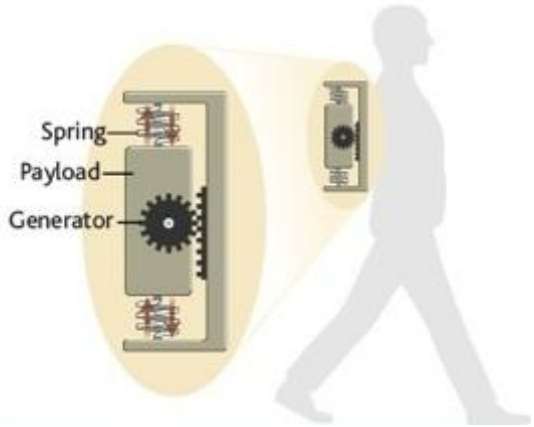

Figure 1.1 : Energy harvesting backpack [5]

It is claimed to obtain 4 *watts* of power while carrying a 29 *kg* payload with the energy harvesting backpack. The result is very noticeable. Indeed, it is much higher than the power levels obtained with the methods mentioned previously.

Moreover considering the range of horizontal distance which legs travel it is suitable to design a linear generator for harvesting energy. In one of the attracting studies, a linear generator sited at the sides of shoe as shown in Figure 1.2 recovers power from horizontal foot motion. It is claimed to recover 70-90 *mW* of average power by the traveler with the mechanism shown in Figure 1.2.

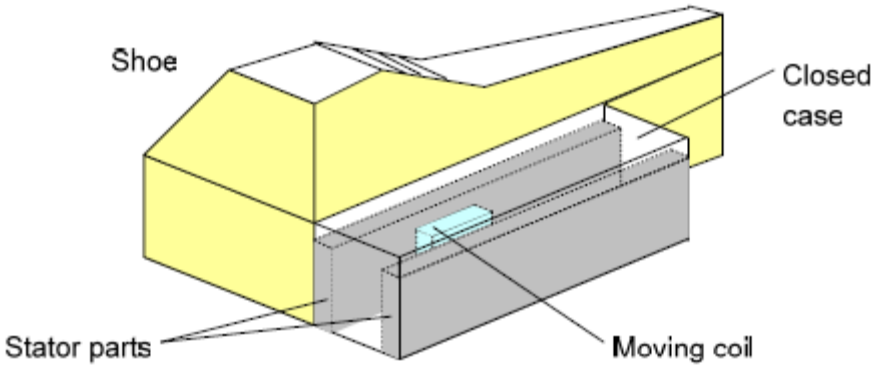

Figure 1.2 : Foot motion sliding generator [6]

In this thesis, the methods suggested for human energy harvesting are evaluated based on the simplicity of the design, efficiency and metabolic cost for user. Taking into account of these parameters, it will be offered two designs for energy harvesting from leg motion, which have been studied throughout of this thesis. In the first type of design rotor is made of laminated iron with winding around it hanged on one of the legs. Stator with strong permanent magnets *(NdFeB)* hanged on the other leg. Then *emf* induces as one leg passes next the other leg when walking. Second type generator design is similar to the first type in the basis of its rotor and stator design. However, this time it has an integrated design in which both rotor and stator are in a single build, which is placed on leg. In both methods, energy is harvested from continuous periodical winding flux change by the movement of legs.

1.1 Need For Energy Harvesting

The number and variety of portable electronics have been increasing rapidly for the last two decades [1]. Laptops, cellular phones, digital assistants, MP3 Players, I-Pods are the most popular portable electronics being used in the world. Today a research announced by International Telecommunication Union reveals the growth of usage of cellular phones around the world in the last decade as shown in Figure 1.3. With the increase in number, functionality of a cellular phone has increased as well. Today a cellular phone can be integrated with camera, radio, and GPS etc. functionality. In addition, in many countries having 3G and 4G supporting networks, cellular phone users have capabilities of high-speed data transfer over internet. Therefore, it is obvious that human being is going to be more and more dependent to live with portable electronics.

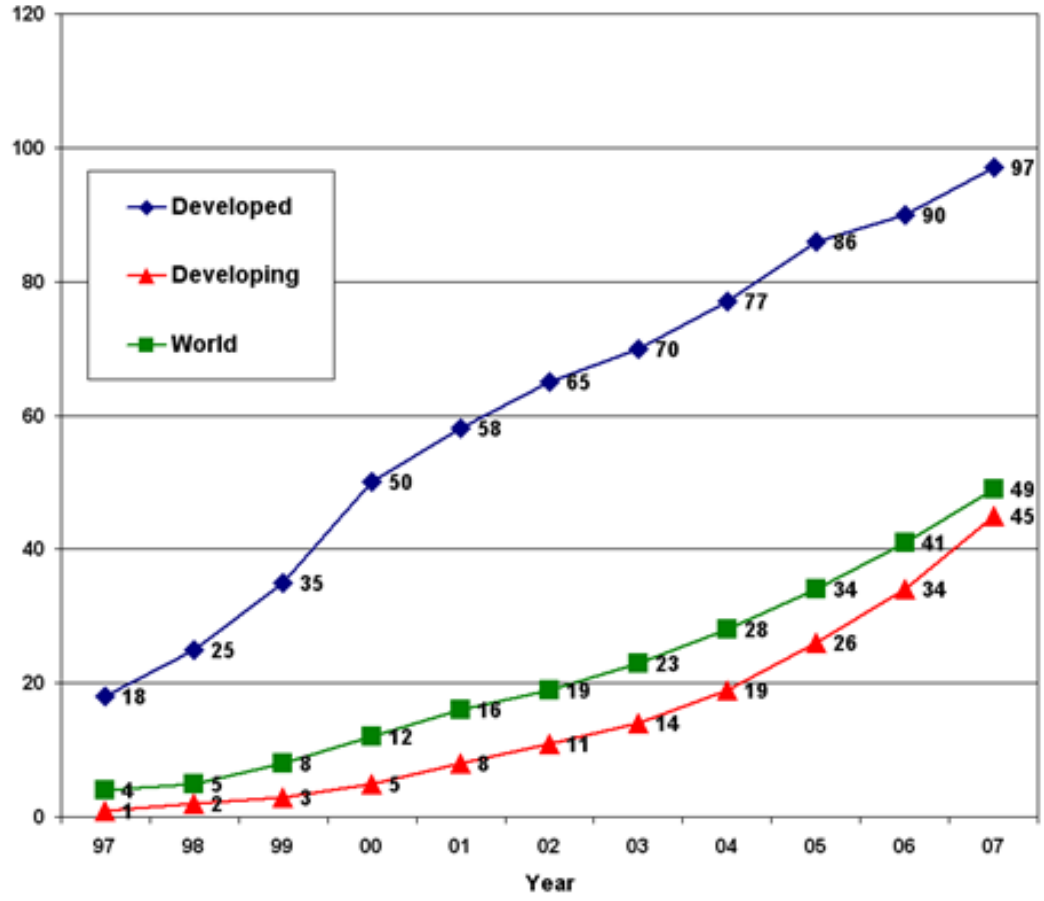

Figure 1.3 : Mobile phone subscribers per 100 inhabitants 1997-2007 [1]

It is a common thought that the most desirable thing for a portable electronic device is being lightweight and having durable operation. Batteries used in portable electronics capture a considerable rate of total weight. Therefore, it seems that manufacturers should consider on inserting light, high efficient and more durable batteries in mobile devices. In Figure 1.4, the improvements of technologies used in a laptop over years are shown in logarithmic scale [1]. As it is shown while the CPU speed increased 1000 times from 1990 to 2002, the energy density of the battery used increased only 3 times. Nonetheless, it has been enabled battery powered electronics to live longer by the technological improvements on integrated circuit design and by employing highly developed power management architectures. However, this is not sufficient to close the gap for energy density of batteries when considering the increase in expectations of human beings from portable electronics. It is studied on another option for many years for sustaining more durable power to portable electronics, human-powered energy sourcing.

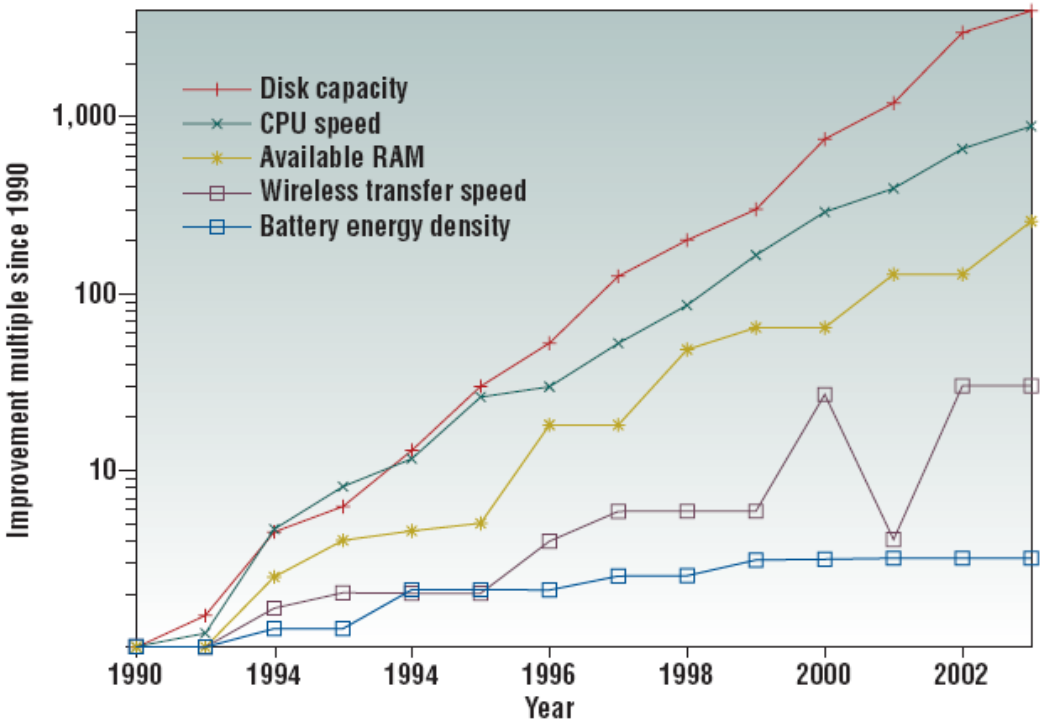

Figure 1.4 : Improvements in mobile computing technology from 1990-2003 [1]

1.2 Human Is An Energy Source

Human body consumes energy of 70 to 1400 *Kcal per hour* in daily activities. On the other hand, a trained athlete consumes 9500 *Kcal per hour* for short bursts [7]. Average power requirements for daily activities of human are shown in Table 1.1.

Table 1.1: Human body activities vs. power requirements [1]

Activity	*Kilocal/hr*	*Watts*
Sleeping	70	81
Lying quietly	80	93
Sitting	100	116
Standing at ease	110	128
Conversation	110	128
Eating a meal	110	128
Playing violin	140	163
Housekeeping	150	175
Carpentry	230	268
Hiking, 4 mph	350	407
Swimming	500	582
Mountain climbing	600	698
Long-distance running	900	1048
Sprinting	1400	1630

In addition, power requirements for some portable electronics are shown in Table 1.2.

Table 1.2: Power consumption of some portable electronics [8]

Products	Power Consumption in stand-by mode (Watts)	Power Consumption in active mode (Watts)
Two way communicator	0.042	1.7
Cellular phone	0.158	0.675
Pagers	0.023	0.030

As it is seen harnessing a small amount of power from such activities is sufficient to operate some of portable electronics.

Henceforward's available energy harvesting sources of human activities such as body heat, breathing, walking are mentioned. Calculations for possible power outputs are given for these activations. Then it is evaluated the feasibility of energy harvesting from these activities.

1.2.1 Body Heat

During the processes held in human body, it is dissipated some considerable energy as heat. It can be used Carnot[1] efficiency for calculating the amount of heat energy occurred because of body activities. In [7], the below calculations made for obtaining the power levels generated as a result of human body activities. For example, if a person in a room of $20\,^{\circ}C$ temperature Carnot efficiency is;

$$\frac{T_{body} - T_{ambiant}}{T_{body}} = \frac{(310K - 293K)}{310K} = 5.5\% \qquad \textbf{(1.1.a)}$$

T_{body} : Body temperature

$T_{ambiant}$: Room temperature

If the room temperature is increased to $27\,^{\circ}C$ Carnot efficiency drops to;

$$\frac{T_{body} - T_{ambiant}}{T_{body}} = \frac{(310K - 300K)}{310K} = 3.2\% \qquad \textbf{(1.1.b)}$$

[1] Carnot cycle is a particular thermodynamic cycle.

Using these values, it can be calculated net generated power from the activity of sitting. According to Table 1.1 $116W$ power is expended during sitting. Multiplying this value with the Carnot efficiency values found above the recovered power is found $3.7W$ and $6.4W$ respectively. However due to some biological events happening in the body that recovered power diminishes further. The main causes for this diminished power are the perspiration of skin and constriction of blood vessels at the parts of body facing with cold air. In fact, by these two events the temperature on that part of the skin decreases resulting Carnot efficiency to drop. To reduce the effects of these events a design can be built to recover power from neck or head as high amount of blood transfer occurs in that parts of the body. Then a rough estimate can be made about the generated power from neck or head by multiplying the ratio of covered area by neck or head to the whole body.

To conclude, in spite of high amount of heat energy generated during the activities of human body this method of harnessing power is unsuitable for two main reasons. First, one is that the efficiency of energy harvesting system is very unstable due to changes in environment temperature. Secondly, an energy harvesting system recovering heat energy from neck or head is not comfortable for the user.

1.2.2 Breath

An average person of 68 kg has an approximate air intake rate of 30 *liters per minute* [9]. The breath pressure is approximately 0.2% above the atmospheric pressure [7]. To escape from the physiological effects only exhalation is considered for recovering energy. Then the available power can be calculated.

$$P = p\Delta V = 0.02 \times \left(\frac{1.013 \times 10^5 kg}{m.sec^2}\right) \times \left(\frac{30l}{1min}\right) \times \left(\frac{1m^3}{1000l}\right) = 1W \quad \textbf{(1.2)}$$

P : Power (W)

p : Air pressure at sea level: $Pascal = \left(\frac{kg}{m.sec^2}\right) \rightarrow 1.013 \times 10^5 kPa$

V : Volume (m^3)

If the activity of a person differs the calculated power from Equation 1.2 changes as well. It is suggested using air masks as pilots to increase the breath pressure [2]. However, a combination of turbine and generator system yields an efficiency of approximately 40% [7].

Therefore, it is not feasible to harvest power from breath as its low efficiency and unacceptable physiological effects on user.

Another way of harvesting energy is from the motion of chest while breathing. A patented mechanism [10], which user fastens around his chest, is shown in Figure 1.5.

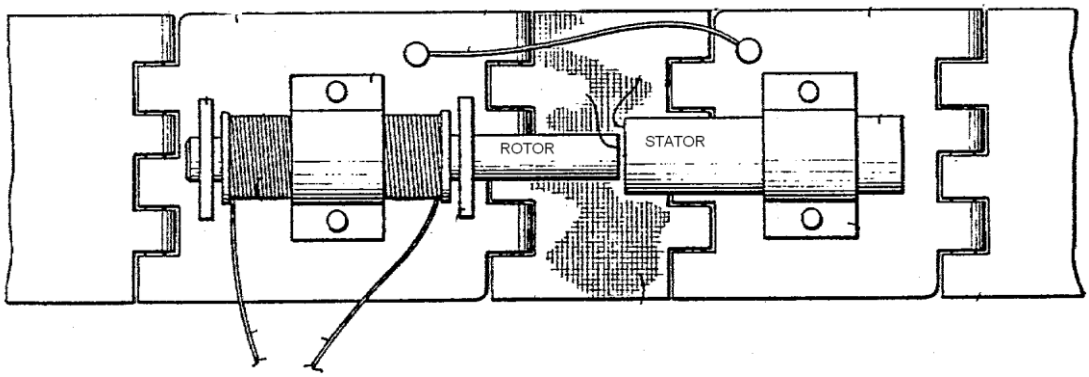

Figure 1.5 : Tight band fastened around chest [10]

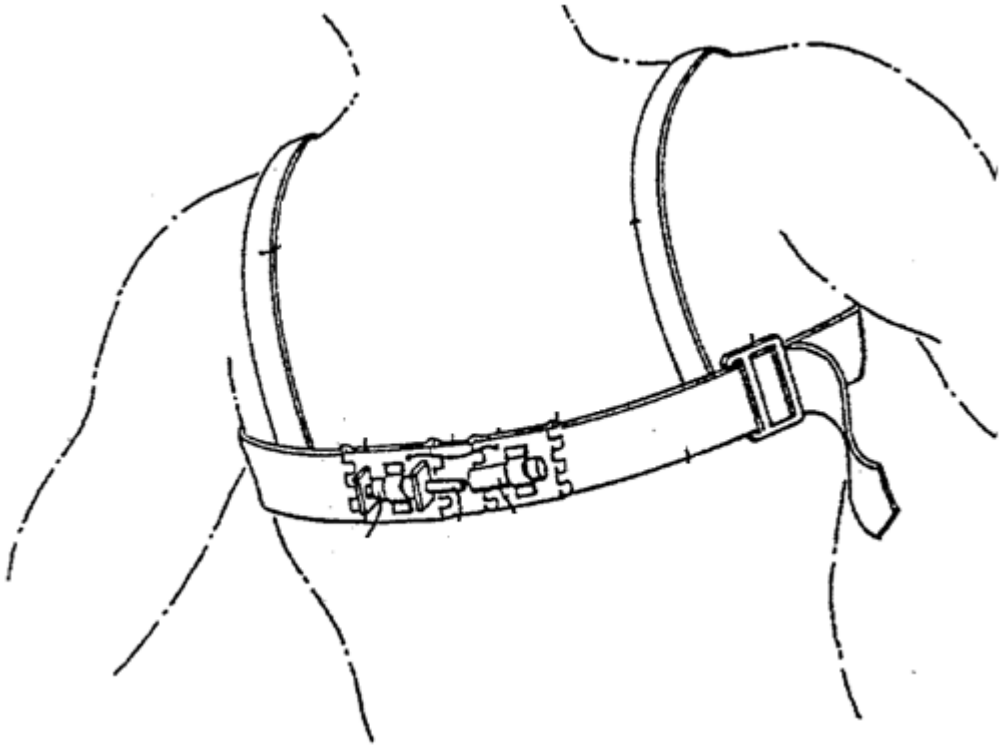

Figure 1.6 : Tight band fastened around chest on user [10]

The working principle of this mechanism is based on electromagnetic energy conversion. As shown in Figure 1.5 rotor is made of a permanent magnet material with winding around it and stator is made of a ferromagnetic material. When the user

breathes in and out, the rotor and stator come up and draw away which induces *emf* at the winding terminals. The difficulty of breathing when carrying this mechanism makes it unpractical to use as an energy-harvesting instrument.

1.2.3 Blood Pressure

Assuming average blood pressure of human is $100\,mmHg$, a hearth rate of 60 *beats per minute* and hearth stroke volume of $70\,ml$ through the aorta per beat [11] the generated power is to be;

$$100\ mmHg \times \left(\frac{1.013\times10^{5}\ kg/m.\sec^{2}}{760\ mmHg}\right)\times\frac{60\ beats}{1\ min}\times\frac{1\ min}{60\ sec}\times\frac{0.07\ l}{beat}\times\frac{1\ m^{3}}{1000\ l} \qquad \textbf{(1.3)}$$
$$= 0.93\ W$$

This technique for energy harvesting can be benefited in medical applications. If a small fraction of this power is harnessed it is obtained enough power to operate low-power microprocessors used in medical sensors and prostheses.

1.2.4 Walking

Walking is one of the most energy consuming motion type held by the body. In fact according to [9] a $68\,kg$ man walking fast at two steps per second consumes $324\,W$ of power. Furthermore, during walking many types of motion take place, which make suitable to harvest energy from walking. These are sole bending, heel strike, knee twisting and horizontal.leg and arm motions. As it is mentioned in the previous section, heel strike is the most noticeable motion type, which is studied on about human energy harvesting. The power generated by the fall of the heel through 5 *cm* can be calculated as,

$$P = F.v = (68kg)\times\frac{9.8m}{\sec^{2}}\times\frac{2steps}{\sec}\times0.05m = 67W \qquad \textbf{(1.4)}$$

P : Power (W)
F : Force (N)
v : Speed (m/sec)

This huge amount of power obtained shows why most of the human energy harvesting studies are based on heel strike motion.

In addition, legs exhibit a large range of motion while walking, which makes possible to design a linear generator as an energy-harvesting device. Therefore, it is worth to calculate the power generated from the horizontal movement of leg.

Roughly, speed of legs moving horizontally is varying sinusoidally. Hence, horizontal speed of leg can be expressed as,

$$v(t) = A \times sin(2\pi \frac{t}{T}) \quad \textbf{(1.5)}$$

where,

v: speed(m / sec)
A: Constant
T: period of one step(sec)
t: time(sec)

from which acceleration

$$a = \frac{dv}{dt} = A \times \frac{2\pi}{T} \times \cos(2\pi \frac{t}{T}) \quad \textbf{(1.6)}$$

is obtained. Assuming walking at 2 *steps/sec* and one-step is 0.75 *m* long, *A* is found 2.35 by using the equation (1.7).

$$\int_0^{0.5} v \times dt = 0.75m \text{ at } T = 1 \; sec \quad \textbf{(1.7)}$$

Now the power generated can be found by replacing Eq. (1.5) & (1.6) in Eq. (1.8). Then maxima and minima values of the power can be obtained by equating the derivative of power to zero.

$$F = m \times a = 10 \times 2.35 \times 2\pi \times \cos(2\pi t) \cong 148 \cos \omega t \; N$$
$$P = F \times v = (148 \cos 2\pi \frac{t}{T}) \times (2.35 \sin 2\pi \frac{t}{T}) \cong 347 \cos 2\pi \frac{t}{T} \times \sin 2\pi \frac{t}{T} \; W \quad \textbf{(1.8)}$$

where,

F : Force(N)
m : Assumed leg weight(kg)
P : Power(W)

$P_{\min} = 0$ and $P_{\max} = 174W$ is found

It is seen that the amount of the generated power from horizontal leg motion is far above the other motion types. Therefore, it is convenient to choose walking as the primary energy harvesting motion type. In the following chapter, some of the available designs [1-6] in literature are reviewed which are made for harvesting energy from walking and two new models are offered which have been studied throughout this thesis study.

2. WALKING AS AN ENERGY SOURCE

As found in the last section, the power generated from the motion of walking is much bigger than the obtained power from the other body motions. Furthermore, many motion types taking place at legs such as knee moving, heel strike etc. make it possible to design various energy harvesting techniques. Moreover and the most important thing is that user carrying a power harvesting tool on his legs has much less serious physiological effects on him than harvesting power from other body motions.

In literature, most of the studies about power harvesting from heel strike motion are based on using piezoelectric materials. Furthermore, there are several designs built based on capturing energy by electromagnetic induction or electromechanical conversion using a gear mechanism [1].

In this section, from literature some energy harvesting studies based on vertical heel strike motion and horizontal leg motion are investigated. In addition, these methods are evaluated by their pros and cons for their feasibility to use.

2.1 Energy Harvesting- Making Use of Vertical Foot Strike Motion

Piezoelectric materials generate electric charge when compressed or bend. Quartz, human skin and bone are the examples of materials with this property. A graphical representation of piezoelectric material is shown in Figure 2.1.

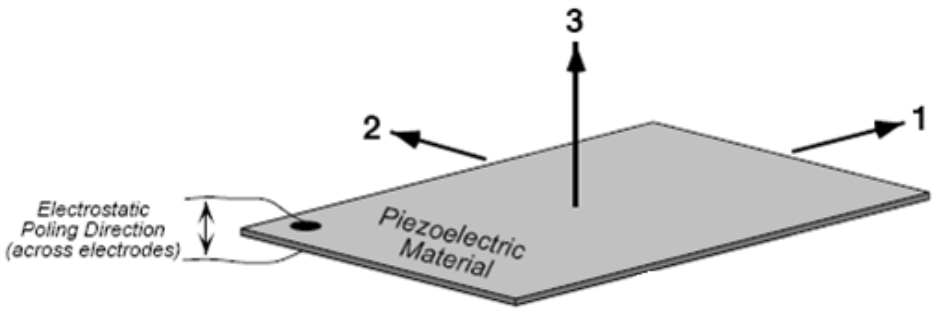

Figure 2.1 : Piezoelectric material sheet

A piezoelectric material has modes of operation at three axes. Mode *XY* means applying electric potential difference across *X-axis* results in stretching/shrinking of the piezo material across *Y-axis* and vice versa. For example, when a mechanical stress applied through axis 3 polarization of electric charges occurs through axes 1, 2 and 3. Also this operation is reversible. That is, when it is applied electric potential difference across axis 3 it results stretching/shrinking or bending (according to the direction of polarization) of the piezoelectric metal through axes 1-3.

There are two common piezoelectric materials. Polyvinylidene fluoride (*PVDF*) and lead zirconate titanate (*PZT*) used in industry of which some properties are shown in Table 2.1.

Table 2.1: Characteristics of *PVDF*&*PZT* [7]

Property	Units	PVDF	PZT
Density	g/cm^3	1,78	7,6
Relative permittivity	ϵ_r	12	1700
Elastic modulus	$10^{10} N/m$	0,3	4,9
Piezoelectric constant	$10^{-12} C/N$	d_{31}=20 d_{33}=30	d_{31}=180 d_{33}=360
Coupling constant	*CV/Nm*	0,11	k_{31}=0,35 k_{31}=0,69

In the table, piezoelectric constant for the relevant mode[2] shows the capacity of charge generation per applied force and coupling constant for relevant mode[3] shows the ability of electromechanical energy conversion. Elastic modulus is the resistance of piezoelectric material to compression. From Table 2.1, using *PZT* at mode 33 has the biggest energy conversion ratio. However, it is not so easy for *PZT* to generate electric charges by working at mode 33. This can be shown by Eq. (2.1) [1].

$$\Delta H = \frac{FH}{A\gamma} \qquad \textbf{(2.1)}$$

Where F is applied force, H is unloaded height, A is area of applied force, γ is elastic modulus constant $(4.9\times10^{10} N/m^2)$ and ΔH is the change in height of *PZT*. A calculation can be made to see the results of working piezoelectric material at

[2] d_{XY} is the piezoelectric constant for XY mode of operation.
[3] k_{XY} is the coupling constant for XY mode of operation.

mode 33. Assuming a man weighing 68 *kg*, has *PZT* inserted to his shoe sole with dimensions of 0.002 *cm* thickness and $100\,cm^2$ area (area of a shoe sole). Inserting these values in Formula 2.1 $\Delta H = 0.23\times10^{-8}\,cm$ is obtained. Then, according to Eq. (2.2) recovered energy from heel strike motion will be very small when operating *PZT* at mode 33.

$$W = F \times \Delta H \qquad \textbf{(2.2)}$$

Thus operating a piezoelectric at mode 33 that is used for energy harvesting from heel strike is useless. However, it is more suitable to use mode 31 for energy conversion. At this mode if the piezoelectric material bends toward axis 3 electric potential is generated through axis 1.

As elasticity of unprocessed piezoceramic sheet, which is a kind of *PZT* material, is low, it is not suitable for applications where flexibility is necessary like energy harvesting from foot bending.

PVDF on the other hand is very flexible. There is a patented design [1] where *PVDF* sheets used for capturing energy from ocean waves. From an industry representative [12], it is known that a 116-cm^2 40-ply $(28\mu m\times 40 = 1.1mm)$ triangular plate with a center metal shim deflected 5 *cm* by 68 *kg* 3 times every 5 seconds results in the generation of 1.5 *W* of power.

In [7], it is made a relationship between the experiment of energy harvesting from ocean waves and energy harvesting from sole bending using *PVDF* sheet as follows. To make a similarity, footprint of a human can be taken 116 cm^2. Besides, it is known that the effective force applied by the shoes when walking is about 30% higher than the traveler's weight [1]. Therefore, it is sufficient to take a person weighing 52 *kg*. The remaining thing to be considered is the walking speed, which is taken 2 *steps/sec*. Then scaling the previous 1.5 *W* it is

$$(1.5W)(\frac{2steps/\sec}{0.6steps/\sec}) = 5W$$

obtained. The result is encouraging to make a *PVDF* inserted shoe design for recovering energy from walking. However, the previous 5 *W* power is obtained by doing normalization with the result obtained from ocean wave experiment. There are some other operating conditions, which affect the power obtained. As shown in Eq.

2.3, a more accurate formula that accounts for the displacement current delivered to a load from the strain of a bending piezoelectric element is given in [1].

$$P_{peak} = \frac{(e_{31} A S_1 w)^2 R}{1 + w^2 C^2 R^2} \quad \textbf{(2.3)}$$

Where,

P_{peak} : Peak power produced in *Watts*

e_{31}: Piezo Stress Constant = $d_{31}Y$, where d_{31} is the Piezo Strain Constant and Y is Young's Modulus

A: Total area of the piezoelectric material (the area of the stave scaled by the number or piezoelectric layers)

w : Dominant angular frequency of excitation

R: Load resistance

C :Total capacitance of all piezoelectric layers (note that all layers are connected in parallel to minimize the stave impedance and layers on opposite sides of the centre need to be electrically reversed to account for the opposite strain, hence change in polarity): $C = \varepsilon \frac{A}{t}$

$\varepsilon = \varepsilon_0 \times \varepsilon_r$: Dielectric constant of piezoelectric element

t : Thickness of one layer

S_1 : Net strain along axis 1: $S_1 = \frac{h\Delta y}{(\frac{1}{2}L)^2}$

h : Thickness of the stave

Δy Maximum bending deflection of the stave

L : Length of stave along the bending direction (axis 1)

Plugging the numbers above in Equation (2.3), together with an expected $3\mu F$ stave capacitance and a dominant frequency of roughly 5 Hz (as seen in waveforms taken with people walking on similar piezoelectric insoles [12]) and applying a matching

load resistance that delivers the most power at this excitation frequency (note that this occurs when the denominator of the relation for is 2), it is obtained $P_{peak} = 2.5\ W$.

However the average power is about a factor of five lower than this, as the walking speed is 1 *Hz* per leg. In addition, 5 *Hz* pulse is produced once per step per shoe in a standard 1 *Hz* per leg gait, yielding average power of 250 mW for one such shoe.

However as it is mentioned in [7] this power level, is based on several unwarranted assumptions. A 40-ply *PVDF* stave risks suffering differential, slippage between layers, hence lowering the amount of actual strain. Also, 5 *cm* deflection (Δy) is not realistic, as the bulk of the bending in a shoe sole occurs in a limited area under the metatarsals, hence the strain is not distributed evenly.

An experiment held in MIT Media Laboratory [13], where a laminate of piezoelectric foil, shaped into an elongated hexagon is used, as shown in Figure 2.2.

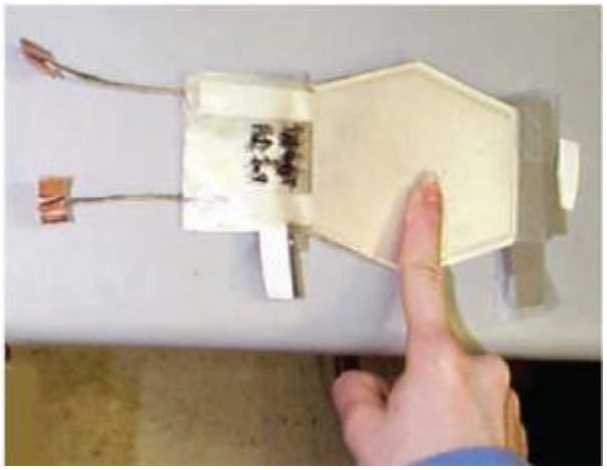

Figure 2.2 : *PVDF* shaped into elongated hexagon

The stave used is a bimorph built around a central 2 *mm* flexible plastic substrate, atop and below which are sandwiched 8-layer stacks of 28-micron *PVDF* (polyvinylidineflouride) sheets, epoxy-bonded. Then it is claimed [13] to have obtained 16 mW peak and 1.3 mW average power at 250 $k\Omega$ load. It is seen that this power level is far below the calculated power levels previously. As mentioned previously the main reason for this difference between experimental and calculated power values is that bending of stave occurs only in a limited area.

In addition, in literature there is another application made by making use of heel strike motion [1]. This time it is used a modified piezoceramic material (*PZT*) for

sustaining flexibility where a unimorph strip of spring steel bonded to a patch of piezoceramic material.

Then operation mode 31 is used for electromechanical energy conversion. It is obtained 1.8 mW of average power achieving to energize a RF transmitter, which is able to transmit 12-bit ID code [1]. In Figure 2.3, it is shown the photography of the last two designs.

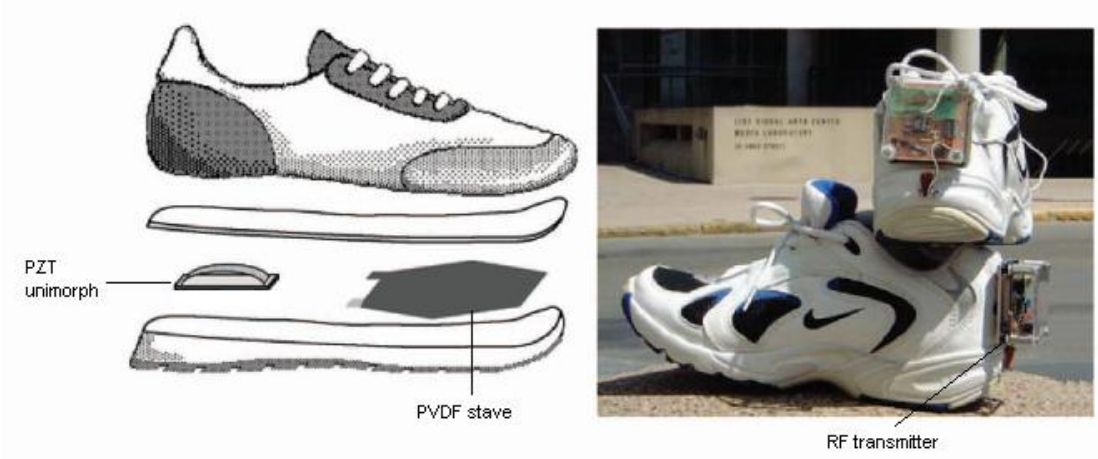

Figure 2.3 : *PVDF*& *PZT* used designs energizing RF transmitter [1]

2.2 Energy Harvesting- Making Use of Horizontal Leg Motion

When walking it is exhibited large range of motion and legs drive big forces. Therefore, it is feasible to design an electromagnetic generator taking the advantage of horizontal leg motion. Since legs exhibit horizontal motion when walking, it is suitable to design a linear electromagnetic generator to harvest energy. In this section, it is investigated a study from literature, which aims to harvest energy from horizontal foot motion.

2.2.1 Foot Motion Sliding Generator

As calculated in Section 1 about 170 watts of power is produced from the horizontal movement of legs, which makes it suitable for energy harvesting from horizontal leg motion. A study held in literature where a foot motion sliding generator captures energy from horizontal foot motion while walking [6]. The drawing of this generator is shown in Figure 2.4. In this design, to increase the induced emf it is used many poles by implementing several $NdFeB$ type hard magnetic material couples. Rotor

consists of windings on plastic body to eliminate the magnetic field force on it created by stator. Therefore, while this generator is capable of inducing enough *emf* it gives so little burden to user to carry it. At gait speed of 3 *step/sec* it is claimed to obtain $27V$ peak *emf* as shown in Figure 2.5. After regulating the generators' output voltage, it is claimed to deliver $11.7V$ Li-ion battery with an average power range of 70-90 mW.

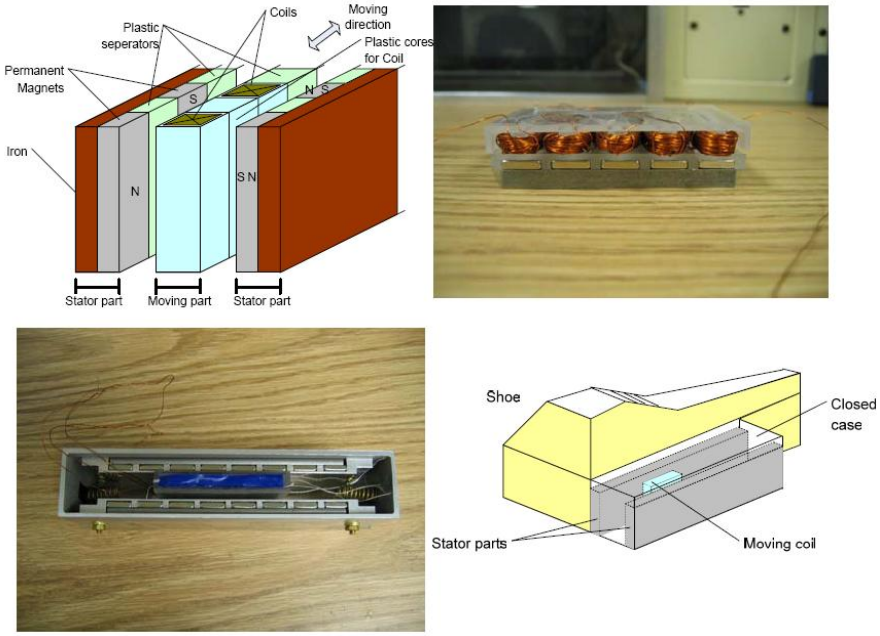

Figure 2.4 : Foot motion sliding generator

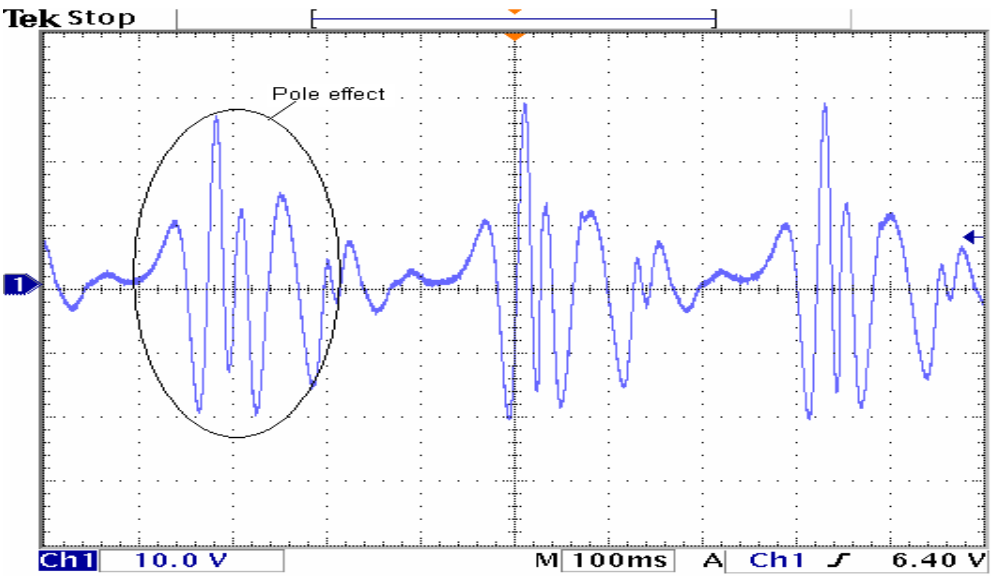

Figure 2.5 : Open circuit voltage of Foot Motion Sliding Generator

When it is investigated the waveform, besides the sinusoidal component at gait frequency (3 *step/sec*) there is another sinusoidal component originating from usage of many poles in generator. In fact, the induced emf can be expressed as in Eq. 2.4.

$V = A \times \sin(wt) \times \sin(kwt)$
$w:$ radial frequency of walking
$k:$ total # of pole **(2.4)**
$A:$ Coefficient depends on the generator properties
(air gap, # of turns, walking speed)

Finally, the feasibility of the last design type can be evaluated As it is shown in Figure 2.5, obtaining a high amount of induced emf eliminates the problem of rectifying and regulating the output voltage of the generator. Also, rotor core is a nonmagnetic material which makes it easy to move the rotor inside while giving less labor to user. However, being a nonmagnetic material of rotor core results in winding not to completely link the magnetic fields. In fact, this reduces the amount of induced emf considerably.

After investigating some of the designs in literature it can be concluded that an energy harvesting device should be well designed to scavenge enough energy with giving little burden to carrier as possible.

Then, in the next chapter, it is proposed two novel designs, which aim to harvest energy from horizontal leg motion.

3. NOVEL ENERGY HARVESTING GENERATORS BASED ON HORIZONTAL LEG MOTION

In this thesis, studies are mostly based on designing an appropriate energy-harvesting device making use of horizontal leg motion. When walking it is exhibited large range of motion and legs drive big forces. Therefore, it is feasible to design an electromagnetic generator taking the advantage of horizontal leg motion. Since legs exhibit horizontal motion when walking, it is suitable to design a linear electric generator to harvest energy. From these facts, in this study it is aimed to build a novel human energy-harvesting device to scavenge enough power to charge the battery of a small portable electronic with giving minimal effort to the user. Therefore, during the thesis process it was studied on two types of novel energy harvesting generators. Firstly, it is considered to build a generator of which stator is at the one leg of a person and rotor is at the other leg. Then by the relative movement of legs to each other it is aimed to induce emf . Secondly, instead of separating rotor and stator from each other, it was considered to build a united form of design placed on one of the legs.

3.1 Rotor and Stator Placed On Different Legs

As mentioned in previous chapters walking is the most suitable kind of motion held in body for energy harvesting issue. Because, as well as providing considerable amount of power be harvested, placing an energy harvesting device to user's leg give insignificant physiological effects to him. Then, studies were on a linear generator design of which stator is at one leg and rotor is at the other leg as shown in Figure 3.1.

The properties of the design are as follows. Rotor is made of an iron core with cupper wire wounded. Stator is built by placing magnetically strong $NdFeB$ type magnets on an iron body. When the carrier walks, electric current induces on the rotor

windings. A prototype with the dimensions shown in Figure 3.2, was built to get an idea about the amount of induced emf at rotor windings.

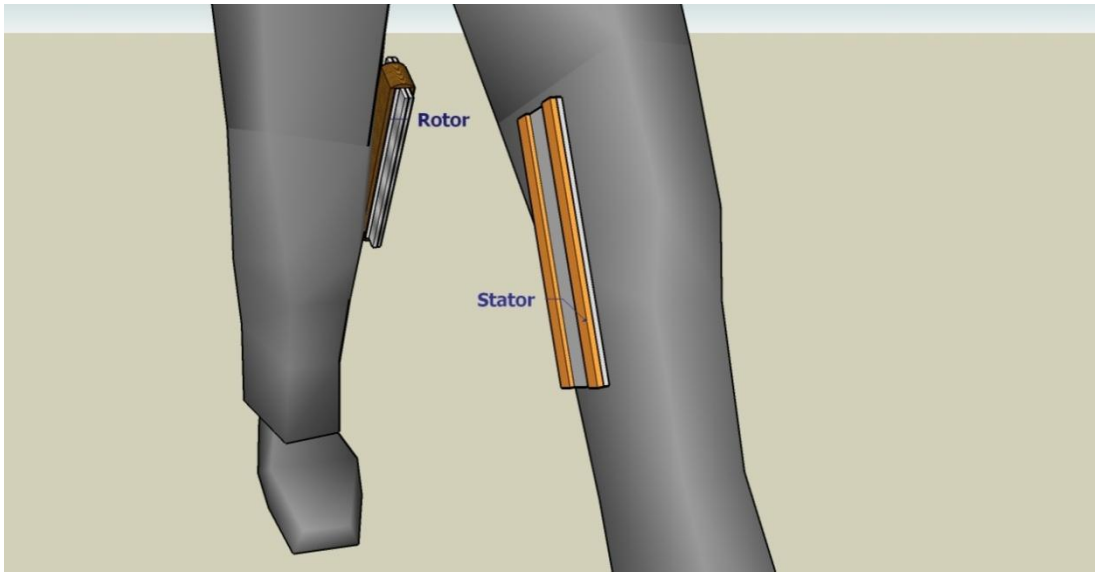

Figure 3.1: Separated Rotor and Stator Generator Design

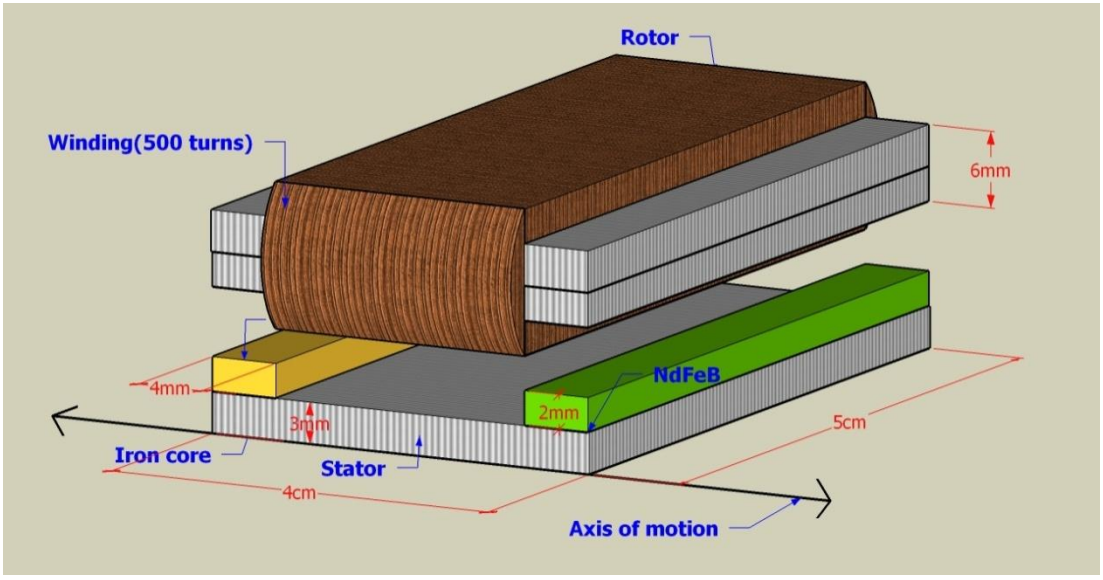

Figure 3.2: Dimensions of the built prototype

The prototype was built on wooden legs. By this mechanism, it is possible to adjust the air gap between rotor and stator and gait speed as well. Adjusting air gap to 2-3 *cm* and walking speed to 5 *steps/sec* following induced emf waveform obtained as shown in Figure 3.3. In fact, it resembles to the waveform shown in Figure 2.5 except the pole effects as it is a one pole generator. It is obtained about $2\,V$ peak and $450\,mV$ *rms* open circuit voltage at about 5 *step/sec* frequency. However, in real life

walking frequency of a human is about 2 *step/sec* with an air gap of about 5 *cm* between legs which causes the induced *emf* to diminish further. As a result, in spite of the fact that the user carrying separated rotor and stator type generator has to make little effort, he is not able to scavenge significant amount of energy.

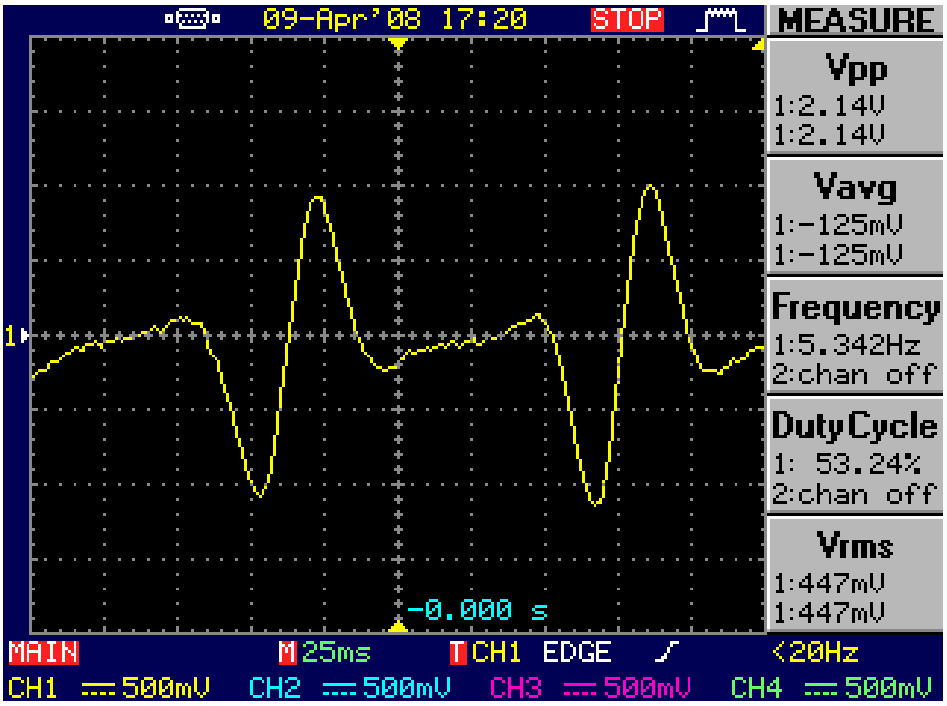

Figure 3.3: *emf* waveform for the generator in Figure 3.2, 500 *mV/div*-20 *ms/div*

3.2 Integrated Rotor and Stator with Iron Rotor Core

This design is very similar to foot motion sliding generator mentioned in Section 2.2.1 except it has an iron rotor core instead. By implementing an iron core, leakage flux is to be reduced significantly and it is possible to induce more *emf* at the rotor windings. However, one must take care of the effects of magnetic forces acting on the rotor. In the design process, it is very important to have deep information about these forces to be confident for the rotor completing its path during walking.

The upper section view of this novel design is shown in Figure 3.4. As seen in the figure, for ease of moving of rotor on its path magnets place in an antisymmetric manner. In fact, antisymmetric build of magnets helps to reduce magnetic forces acting on the rotor. Then, there are two important parameters that should be criticized for the generators' feasibility of use. First parameter is the induced *emf* on rotor winding. Second parameter is the forces acting on the rotor. Therefore, some

calculations should be done to have a view of the amount of *emf* induced and forces acting on the rotor. Here, these calculations are held by the method of finite element analysis (FEM) with the help of FEMM program [14]. The analysis made by moving rotor gradually and getting the results of magnetic and mechanical forces on the rotor and induced *emf* at rotor windings at each step.

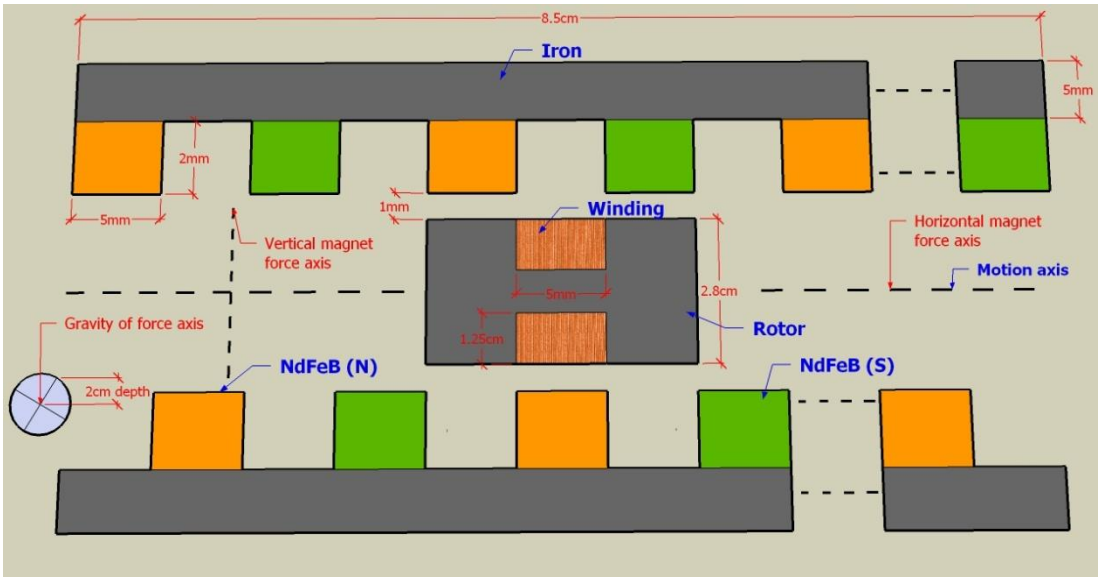

Figure 3.4: Integrated type linear generator design

Before jumping into the FEM analysis results, it will be useful to investigate the variables that affect the amount of induced *emf* and movement of rotor. At this point, it will be useful to draw a free body diagram of the rotor as shown in Figure 3.5.

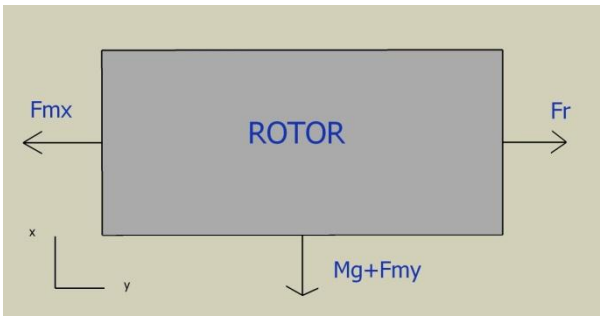

Figure 3.5: Free body diagram of rotor

F_{mx} : Horizontal magnetic force

F_{my} : Vertical magnetic force

F_r : Accelerating force created by acceleration of leg during walking($M_r a_s$)

Mg : Gravity force of rotor
M : Mass of rotor
g : Gravitational acceleration of earth $(9.81 m/s^2)$

The movement of leg creates an accelerating force on the rotor. This force is resisted by horizontal magnetic force and friction force which is created by vertical magnetic force and gravity force of the rotor. Then based on Newton's laws of motion rotor acceleration, speed and position can be expressed as in Eq. 3.1

$F_{net} = F_r - F_{mx} - \mu(F_{my} + Mg)$, Net force on the rotor
μ : coefficient of static/kinetic friction
$F_{net} = M \times a_r$
$a_r = \frac{F_{net}}{M}$, rotor acceleration **(3.1)**
$v_r = \int_t a_r dt,$ rotor speed
$X_r = \int_t v_r dt,$ Rotor position

The calculation steps for stator (leg) position (X_s) and rotor accelerating force (F_r) are as follows:

$v_l = 2$ *steps / sec*- walking speed
$V_r = 3100 mm^3 -$ rotor iron part volume
$V_{cu} = 6000 mm^3 -$ rotor cupper 30 AWG part volume
$d_i = 7.87 g / cm^3 -$ density of iron
$d_{cu} = 8.96 g / cm^3 -$ density of cupper
$M = V_r \times d_i + V_{cu} \times d_{cu} \cong 78g -$ rotor mass
$v_s = A \times \sin(2\pi f)t -$ horizontal leg (stator) speed
$T = \frac{1}{f} = 1\text{sec} -$ period of one leg to complete one cycle
$X_s = \int_0^t v_s dt$ - horizontal leg (stator) position
$X_s = \int_0^t A \times \sin(2\pi f)t$

Assuming one step of a person is about 75 *cm*;

$X_s(t = 0.5) = 0.75 = \int_0^{0.5} A \times \sin(2\pi f)t dt$
$\Rightarrow A = 2.36$

As acceleration is the derivative of speed, acceleration of legs can be defined as;

$$a_s = \frac{dv_s}{dt} \text{ - horizontal leg stator acceleration}$$
$$a_s = A \times 2\pi f \times \cos(2\pi f)t$$
$$a_s = 14.83 \times \cos 2\pi t \quad m/\sec^2$$

Then the force exerted on the rotor by the acceleration of leg can be calculated.

$$M = 78g$$
$$F_r = M \times a_s = 1.16 \times \cos 2\pi t \ N \qquad \textbf{(3.13)}$$

Here, the magnetization forces depend on the rotor position. However, rotor position is the integral of rotor speed and rotor speed is the integral of rotor acceleration, which is also dependent on the net force on the rotor finally. Then, a circular dependency occurs between magnetization forces and rotor position. The circular dependency in these equations can be shown as in Figure 3.6.

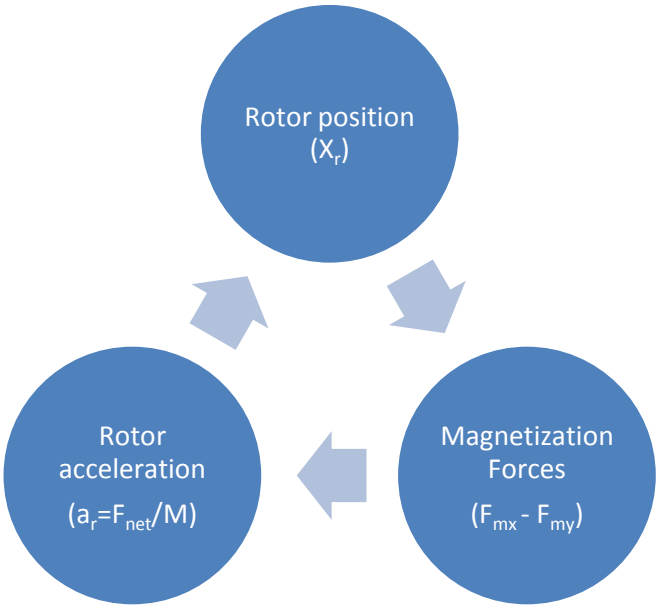

Figure 3.6: Circular dependency between rotor position and magnetization forces

Therefore, some iteration techniques can be used to solve the equations relating rotor position with magnetization forces. However, as shown later we do not need to solve the equations because of the symmetrical structure of the generator. Therefore, some iteration techniques can be used to solve the equations relating rotor position with magnetization forces. However, as shown later we do not need to solve the equations because of the symmetrical structure of the generator.

After specifying the generator dimensions and properties it can be investigated the change of flux and magnetization forces with respect to the rotor position by doing FEM analysis with the help of the FEMM program [14].

FEM analysis can be done for each rotor position (X_r) increased gradually (ΔX_r=0.2cm). A 2D drawing of the generator with about ten thousand meshes inserted is shown in Figure 3.7.

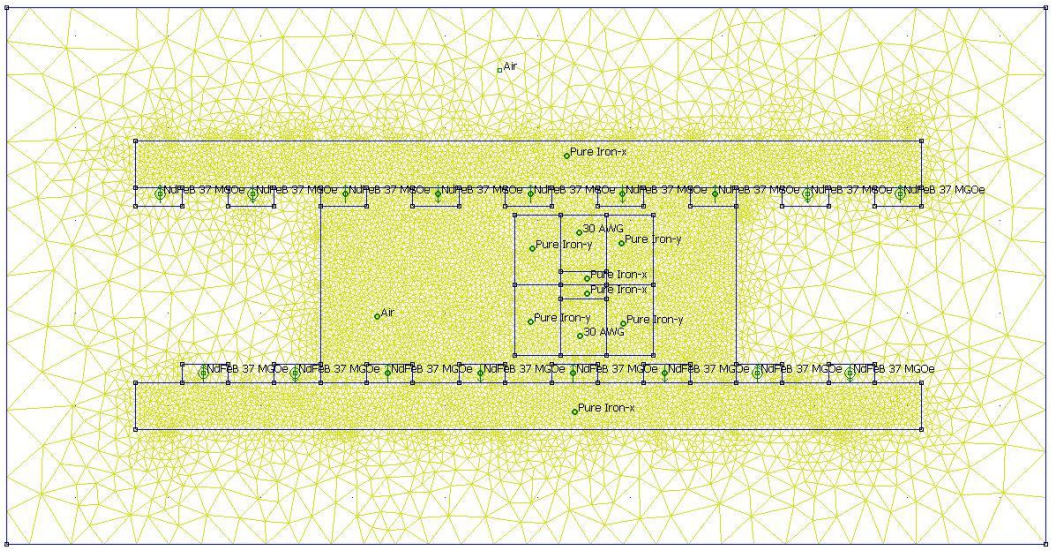

Figure 3.7: Mesh drawing for FEM analysis

In the drawing, it is seen that mesh sizes are drawn smaller in rotor and stator segments and around the rotor than the outside air segment to increase the accuracy of the analysis. Then the resulted magnetic field distributions for some steps (ΔX_r=0.25cm) are shown in Figure 3.8. The linking flux of the rotor winding changes with each step of rotor movement. Here it is seen the magnetic field density (B_r) of the iron rotor core reaches to its maximum value of B_r=1.4 T at X_r=0.25 cm. This proves that there is no saturation of magnetic field density in rotor core. Then it can be calculated the values of rotor winding flux ($\phi_{r\,(X_r)}$), rotor horizontal magnetic force ($F_{mx(X_r)}$) and rotor vertical magnetic force ($F_{my(X_r)}$) at each step. The calculations are computationally intensive. However, symmetrical design of the generator makes it possible to make calculations only for the interval of 1 cm, which is the distance between two poles.

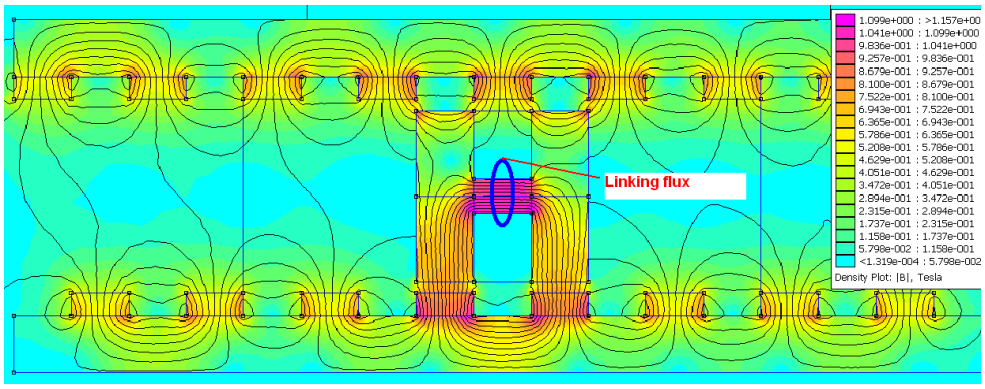

(a)

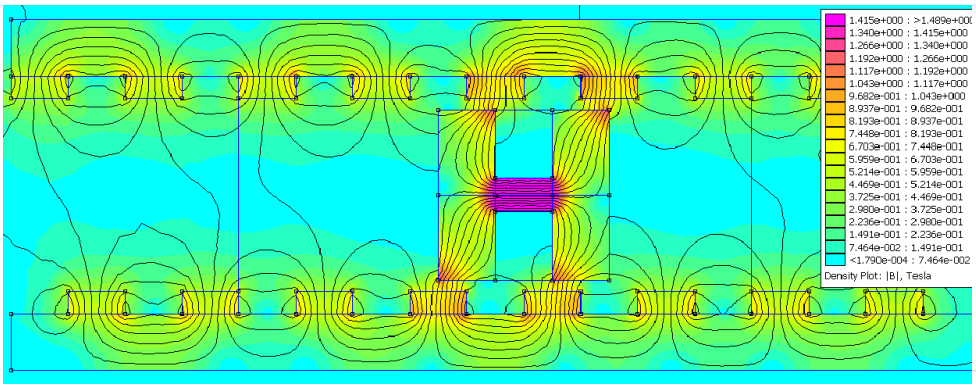

(b)

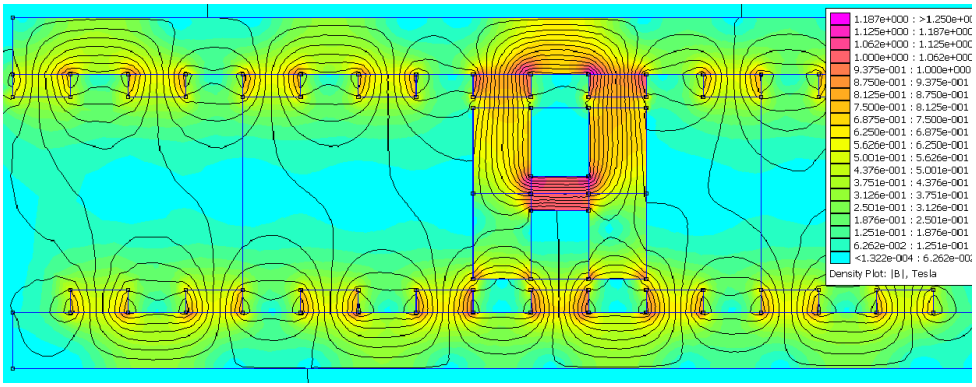

(c)

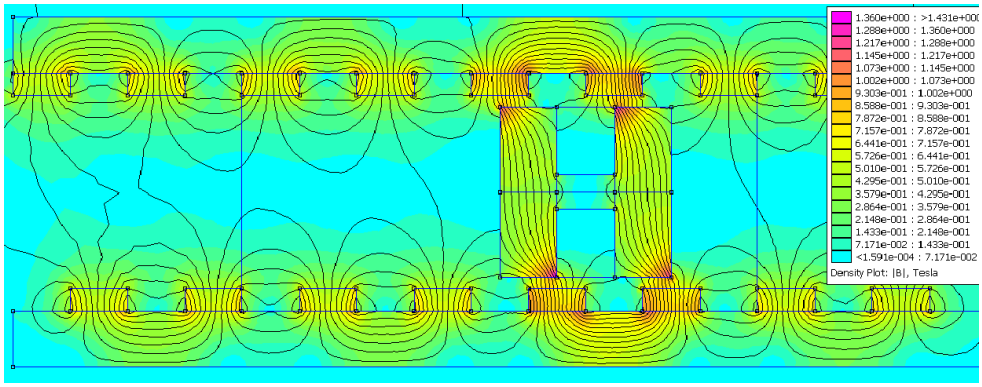

(d)

Figure 3.8: Generator magnetic field distribution for some rotor position (a) X_r=0, (b) X_r=0.25 cm, (c) X_r=0.5 cm, (d) X_r=0.75 cm,

The values of $\phi_{r\,(X_r)}$, $F_{mx(X_r)}$ and $F_{my(X_r)}$ for $\Delta X_r = 0.1cm$ are shown in Table 3.1 and graphical representation of the change of flux and magnetization forces with respect to rotor position is shown in Figure 3.9.

Table 3.1: Winding flux and rotor magnetization force distribution over rotor positions for one pole

Rotor Position	Flux	Magnetizing Force x-y direction	
(cm)	(Weber)	N	
X_r	$\Phi \times 10^{-5}$	F_{mx}	F_{my}
0	6.35	0.37	25.62
0.1	4.01	3.42	19.71
0.2	1.36	1.69	6.79
0.3	-1.3	-1.51	-6.87
0.4	-3.84	-3.58	-19.64
0.5	-6.35	-0.37	-25.62
0.6	-7.69	2.85	-19.52
0.7	-8.73	1.39	-7.13
0.8	-8.75	-1.59	7.19
0.9	-7.97	-3.15	19.57
1	-6.3	0.27	25.62
1.1	-3.96	3.26	19.66
1.2	-1.26	1.55	7.26
1.3	1.38	-1.61	-6.89
1.4	4.03	-3.46	-19.61
1.5	6.37	-0.5	-25.82
1.6	7.76	2.85	-19.52
1.7	8.83	1.39	-7.13
1.8	8.84	-1.59	7.19
1.9	8.1	-3.12	19.6

As it is seen in Figure 3.9, the change of the flux and magnetic forces with respect to the rotor position is sinusoidal. Then horizontal and vertical magnetization forces can be formalized as in Eq. 3.3

$$F_{mx}(X_r) = 3.5\cos(4\pi X_r) \text{ - Horizontal magnetization force}$$
$$F_{my}(X_r) = 25\cos(2\pi X_r) \text{ - Vertical magnetization force} \quad \textbf{(3.3)}$$

In fact, the results for magnetic force and flux change with respect to the rotor position are insufficient to have full understanding of rotor movement and induced *emf* at rotor windings. As shown in Eq. 3.1 rotor position depends on rotor acceleration, which depends on magnetization forces.

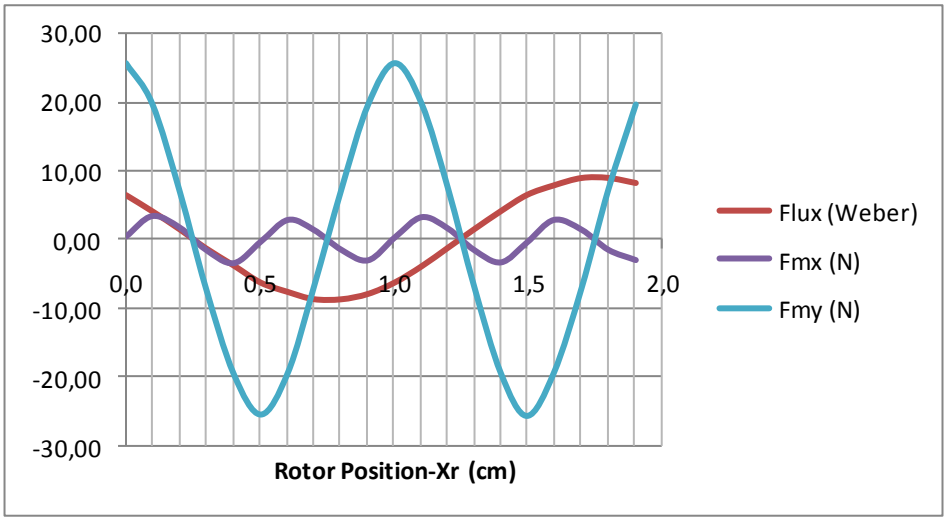

Figure 3.9: Flux and magnetization forces vs. rotor position

Then, a circular dependency occurs between equations. Therefore some iteration techniques should be used to solve the change of magnetization forces and induced *emf* with respect to time and rotor position. However, as found in Eq. 3.3 horizontal magnetization force changes sinusoidally with rotor position, which makes no net effect on rotor position at total. Then we can neglect the effect of horizontal magnetization force on rotor's total travelling time to complete its path. However, the same situation is not valid for the vertical magnetization force since friction force is the absolute of the vertical magnetization force as shown in Eq. 3.4.

$$F_{fr} = \mu \times |F_{my}(X_r)| \text{ , friction force}$$
$$\mu : \text{ friction constant} \qquad \textbf{(3.15)}$$

Therefore in the design process friction force must be decreased as possible as to guarantee the rotor move inside the stator.

Before doing the feasibility check of the generator designed slipping surface type of between rotor and stator should be determined.

Firstly, it is considered to move the rotor over a lubricated iron surface with coefficient of static friction $\mu = 0.15$ read from Table A.1 in Appendix A.1 [15].

After that, a feasibility check process should be performed for the determined dimensions and properties of the generator. It is expected from the generator's rotor to complete its travel before the user walks one step, which is about 0.5 *sec* for a person walking at 2 *step/sec*. In addition, to guarantee the movement of the rotor

average net force acting on the rotor should be positive, shown in Eq. 3.5. Then the feasibility checking process can be schematically represented as in Figure 3.10.

$$F_{net} = F_r - F_{mx} - \mu(F_{my} + Mg)$$

taking average for the time period of rotor completing one pole of movement;

$$\overline{F_{fr}} = \mu \times \overline{(|F_{my}| + Mg)}$$

$$\overline{F}_{mx} = 0 \qquad \textbf{(3.16)}$$

$Mg << \overline{|F_{my}|}$, can be neglected

$$\overline{F}_{net} = \overline{(F_r - \overline{F_{fr}})}$$

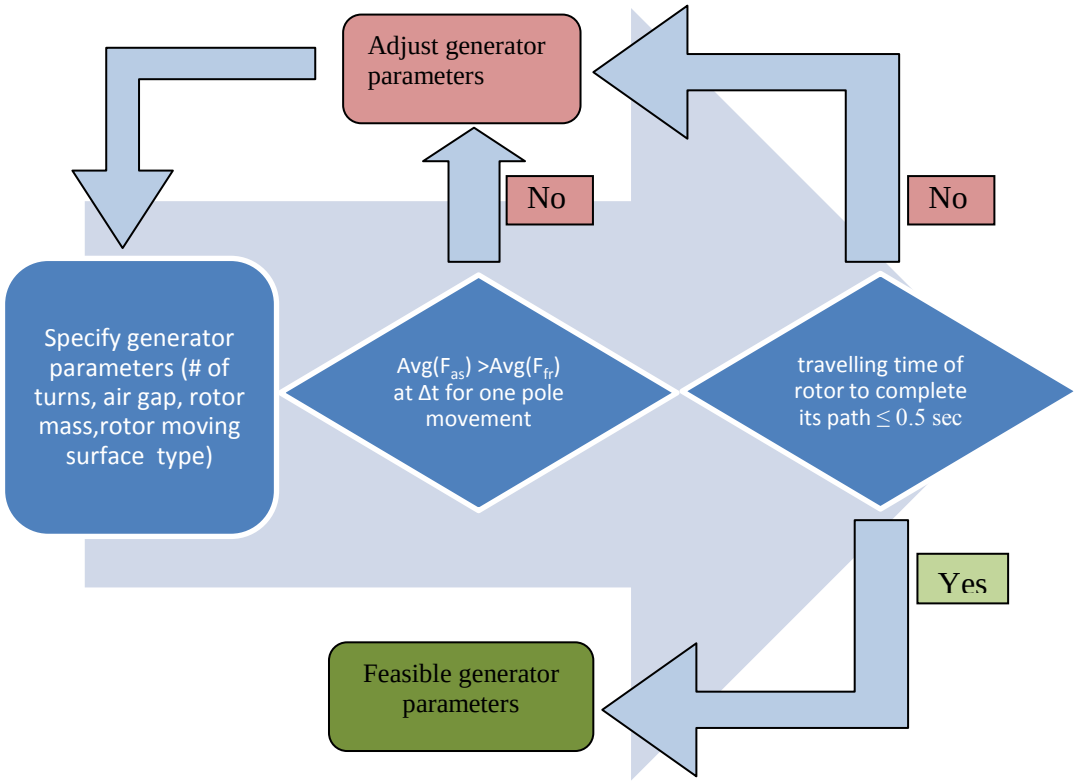

Figure 3.10: Feasibility checking process of designed generator

Now it can be made a feasibility check for the generator parameters. From Eq. 3.2, $F_r = M \times a_s = 1.16 \times \cos 2\pi t \ \ N$ found. Replacing F_r into Eq. 3.6 it is seen that the designed generator is not feasible to implement.

Then, the air gap between rotor and stator is increased to g=2 *cm.* In addition, it is decided to move the rotor on wheels. As a result of this implementation, decrease of both vertical magnetization force (F_{my}) and frictional force (F_{fr}) is possible.

$\overline{F}_{net} = \overline{F}_r - \mu(\overline{F_{my}})$

$\mu = 0.15$ for greasy iron-iron surface

$$\mu(\overline{F_{my}}) = 0.15 \times \frac{2}{\pi} \times 25 = 2.39\ N \quad \textbf{(3.6)}$$

$\overline{F}_r < F_r$ peak =1.16 N

$\Rightarrow \overline{F}_{net} < 0$, feasibility of the generator fails

To calculate the friction force of a wheel Eq. 3.6 must be considered.

$$F_{fr} = \mu \times \frac{W + F_{my}}{R} \quad \textbf{(3.7)}$$

F_{fr} *:* Friction force

μ *:* Coefficient of rolling friction (Iron on iron $\mu = 0.00051m$)[15]

$(\overline{F_{my}})$: Average vertical magnetization force ($\frac{2}{\pi} \times 8.66 = 5.5N$)

W *:* Rotor Weight ($0.078 \times 9.8 = 0.76\ N$)

R *:* Radius of the wheel (1 *cm*)

$\Rightarrow \overline{F_{fr}} = 0.32N$

As it is mentioned previously that rotor position and net force acting on the rotor are dependent to each other. However, if the average values of magnetization forces and friction force considered we are able to approximately find the total travelling time of the rotor. Then we are able to evaluate the feasibility of the generator. The results in Table 3.2 and with detail in Table A.2 given in Appendix A.2 show the movement characteristics of the rotor and stator based on the approximations by taking average values of $\overline{F_{mx}} = 0$ and $\overline{F_{fr}} = 0.32N$. Looking at the shaded part of the Table 3.1, it is seen that rotor completes its path (X_r=8 *cm*) before the leg completes one step of movement (X_s<75 *cm*). Then it is concluded that changing air gap to g=2 *cm* and moving the rotor on a wheel mechanism sustains a feasible generator for energy harvesting.

In addition, the induced *emf* can be obtained by performing iterative calculations for the circular dependency between net force acting on rotor and rotor position. However, Table 3.1 shows that the rotor completes its travel at t=0,13 *sec*, which is considerably smaller than the stator travel time t=0,5 *sec*. Then using the stator position-time change rather than rotor position-time change to calculate the induced *emf* does not result in much differences totally. Therefore, to have an rough idea

about the amount of induced *emf* and its time change we can benefit from Table 3.1. Then, variation of the induced emf with time is obtained as shown in Figure 3.11.

Table 3.2: Movement characteristics of the rotor and stator

Time	Stator			Flux $\times 10^{-5}$	EMF	Force(N)				Rotor		
	Acc.	Spd.	Pos.							Acc.	Spd.	Pos.
t (s)	a_s (m/s^2)	v_s (m/s)	X_s (cm)	Φ (Weber)	V	F_{my}	$\lvert\mu \times F_{my}\rvert$	F_r	F_n	a_r (m/s^2)	v_r (m/s)	X_r (cm)
0	14.83	0	0.00	4.08	0.0	8.66	0.32	1.16	0.84	10.73	0.00	0.00
0.0115	14.79	0.17	0.10	2.65	-1.2	7.07	0.32	1.15	0.83	10.69	0.12	0.07
0.0165	14.75	0.24	0.20	0.87	-3.6	2.59	0.32	1.15	0.83	10.65	0.18	0.15
0.0200	14.71	0.30	0.30	-0.83	-4.9	-2.47	0.32	1.15	0.83	10.61	0.21	0.21
0.0233	14.67	0.34	0.40	-2.65	-5.5	-7.06	0.32	1.14	0.82	10.57	0.25	0.29
0.0261	14.63	0.39	0.50	-4.13	-5.3	-8.66	0.32	1.14	0.82	10.53	0.28	0.36
0.0286	14.59	0.42	0.60	-5.18	-4.2	-6.85	0.32	1.14	0.82	10.49	0.30	0.44
0.0308	14.55	0.45	0.70	-5.70	-2.4	-2.62	0.32	1.14	0.82	10.45	0.33	0.51
0.0330	14.51	0.49	0.80	-5.69	0.1	2.91	0.32	1.13	0.81	10.41	0.35	0.58
0.0350	14.47	0.51	0.90	-5.10	2.9	7.15	0.32	1.13	0.81	10.37	0.37	0.65
0.0369	14.43	0.54	1.00	-4.02	5.7	8.66	0.32	1.13	0.81	10.33	0.39	0.73
0.0387	14.39	0.57	1.10	-2.54	8.2	6.85	0.32	1.12	0.80	10.29	0.41	0.80
0.0404	14.35	0.59	1.20	-0.84	10.0	2.49	0.32	1.12	0.80	10.25	0.43	0.87
0.0420	14.32	0.62	1.30	0.91	10.9	-2.69	0.32	1.12	0.80	10.21	0.44	0.94
0.0436	14.28	0.64	1.40	2.63	10.8	-7.02	0.32	1.11	0.79	10.17	0.46	1.01
.	.	.	.	.	.	.	.	.	.	.	.	.
.	.	.	.	.	.	.	.	.	.	.	.	.
0.1256	10.45	1.68	11.10	-2.54	24.7	6.85	0.32	0.81	0.49	6.34	1.16	7.87
0.1262	10.41	1.68	11.20	-0.83	28.9	2.48	0.32	0.81	0.49	6.30	1.16	7.94
0.1268	10.37	1.69	11.30	0.93	30.4	-2.75	0.32	0.81	0.49	6.27	1.17	8.00

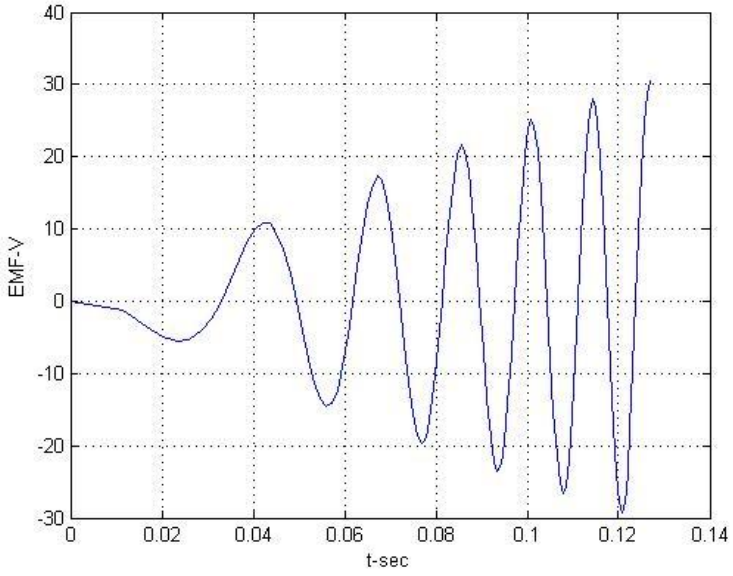

Figure 3.11: Induced *emf* vs. time

4. CONCLUSIONS

The growth of wireless, computing, data storage, communication and display technology has been much faster than energy storage technology. Adapting these growing technologies into portable electronics their power requirement increases as well. Although power management developments enable battery-powered portable electronics to live longer it is not sufficient to meet this growing power requirement.

To close this gap energy harvesting from human motion has been put forward for many years. The practicality of harvesting energy from human motions is evaluated by examining two parameters. First one is, ease of carrying the energy harvesting device designed for that particular human motion. The second is the power level to be scavenged from that motion.

Based on these parameters walking is the most suitable candidate for energy harvesting. In literature, most of the human energy harvesting studies are based on heel strike and bending of foot motions. There are some designs made [16] which captures energy from these motions based on electromagnetic energy conversion principle. However, as an alternative candidate piezoelectric materials are lightweight and easy to shape. Although piezo material has low energy conversion ratio, when it is inserted in a shoe sole the user walking physiology is not disrupted. Therefore, it is the most suitable option for harvesting energy from heel strike or bending of foot.

Horizontal leg motion exhibits a large range of motion, which makes it suitable to design a linear type generator. It is suggested two types of linear generator designs where strong $NdFeB$ type permanent magnets are used. In the first design, stator and rotor are separated and placed on different legs. However, large air gap between legs when walking causes the induced *emf* to be very small. Secondly, an integrated design is suggested which consists both rotor and stator in a unique structure. The generator is placed near the shoe or leg. Contrary to literature study mentioned in Section 2.2, the rotor winding is attached to an iron core to increase the power level as possible.

4.1 Future Work

For the integrated type generator design, the movement of the rotor from one side to other was proved theoretically. Then it must be implemented the generator with the determined properties.

The obtained induced *emf* is an unregulated AC voltage. Based on the obtained induced *emf* it must be designed an effective AC-DC converter to produce a regulated DC voltage with minimum loses. Then most suitable energy storage element should be chosen for effectively benefiting from energy harvesting device.

REFERENCES

[1] Starner T. and Paradiso J.A., 2004 Human Generated Power for Mobile Electronics, in Piguet, C. (ed), Low-Power Electronics, CRC Press, Chapter 45

[2] Url-1 <*http://en.wikipedia.org/wiki/Piezoelectricity*>, accessed at 20.12.2009

[3] Halvorsen.D., 1995 Private correspondence. AMP Inc.

[4] Li Q., Naing V., Hoffer J.A., Weber D.J., Kuo A.D. and Donelan J. M., 2008 IEEE International Conference on Robotics and Automation Pasadena, CA, USA, May 19-23.

[5] Url-2 <*http://www.sciencemag.org/*>, accessed at 10.10.2009.

[6] Niu P. and Chapman P., 2006 Design and Performance of Linear Biomechanical Energy Conversion Devices, Power Electronics Specialists Conference, PESC '06. 37th IEEE

[7] Starner T., 1996. Human Powered Wearable Computing. IBM Systems Journal, Vol. 35, NOS 3&4.

[8] Howells C.A., 2008 Piezoelectric energy for soldier systems, US Army CERDEC C2D Army Power Division 10125

[9] Morton D., 1952 Human Locomotion and Body Form. The Williams & Wilkins Co., Baltimore

[10] Robert J. Hunt, 1981 Chest Motion Electricity Generating Device, US Patent, No: 4245640 dated 01.20.1981.

[11] Braunwald E., Editor 1980 Heart Disease: A Textbook of Cardiovascular Medicine, *W*. B. Saunders Company, Philadelphia

[12] Carroll C.B., 1998 Frequency multiplying piezoelectric generators, US Patent, No: 5814921 dated 03.13.1995

[13] Kymissis J., Kendall C., Paradiso J., and Gershenfeld N., 1998 Parasitic power harvesting in shoes. In IEEE Intl. Symp. On Wearable Computers, pages 132–139

[14] FEMM, A finite element analysis tool, David Meeker

[15] Url-3 <*http://www.roymech.co.uk/Useful_Tables/Tribology/co_of_frict.htm*>, accessed at 29.04.2010.

[16] Duffy M., Carroll D., 2004 Electromagnetic generators for power harvesting, Power Electronics Specialists Conference, PESC 04. IEEE 35th Annual Vol.3 pages 2075-2081

APPENDICES

APPENDIX A 1: Coefficients of Friction of Some surfaces, Adapted from Url-4

APPENDIX A 2: Movement Characteristics of The Integrated Type Designed Generator

APPENDIX A.1

Table A.1: Coefficients of Friction Values For Some Surfaces

Material 1	Material 2	Coefficient Of Friction			
		DRY		Greasy	
		Static	Sliding	Static	Sliding
Aluminum	Aluminum	1.05-1.35	1.4	0.3	
Aluminum	Mild Steel	0.61	0.47		
Bronze	Cast Iron		0.22		
Bronze	Steel			0.16	
Cupper	Cast Iron	1.05	0.29		
Steel	Cast Iron	0.4		0.21	
Cupper	Cupper	1		0.08	
Cupper	Mild Steel	0.53	0.36		0.18
Cupper	Steel		0.8		
Cast Iron	Cast Iron	1.1	0.15		0.07
Chromium	Chromium	0.41		0.34	
Steel (Mild)	Cast Iron		0.23	0.183	0.133
Steel	Cupper Lead Alloy	0.22		0.16	0.145
Steel (Hard)	Graphite	0.21		0.09	
Steel	Graphite	0.1		0.1	
Glass	Glass	0.9 - 1.0	0.4	0.1 - 0.6	0.09-0.12
Glass	Metal	0.5 - 0.7		0.2 - 0.3	
Glass	Nickel	0.78	0.56		
Graphite	Graphite	0.1		0.1	
Graphite	Steel	0.1		0.1	
Cupper-Lead Alloy	Steel	0.22		-	
Iron	Iron	1		0.15	
Lead	Cast Iron		0.43		
Lead	Steel		1.4		
Leather	Wood	0.3 - 0.4			
Teflon	Steel	0.04		0.04	0.04
Teflon	Teflon	0.04		0.04	0.04
Hard Carbon	Hard Carbon	0.16		0.12 - 0.14	
Hard Carbon	Steel	0.14		0.11 - 0.14	
Zinc	Zinc	0.6		0.04	
Zinc	Cast Iron	0.85	0.21		
Wood	Wood (Wet)	0.2			
Wood	Metals(Clean)	0.2-0.6			
Wood	Metals (Wet)	0.2			

APPENDIX A.2

Table A.2: Movement and Magnetization Characteristics of The Integrated Type Designed Generator

Time	Stator			Flux $\times 10^{-5}$	EMF	Force(N)				Rotor		
	Acc.	Spd.	Pos.							Acc.	Spd.	Pos.
t (s)	a_s (m/s^2)	v_s (m/s)	X_s (cm)	Φ (Weber)	V	F_{my}	$\lvert\mu \times F_{my}\rvert$	F_r	F_n	a_r (m/s^2)	v_r (m/s)	X_r (cm)
0	14.83	0	0.00	4.08	0.0	8.66	0.32	1.16	0.84	10.73	0.00	0.00
0.0115	14.79	0.17	0.10	2.65	-1.2	7.07	0.32	1.15	0.83	10.69	0.12	0.07
0.0165	14.75	0.24	0.20	0.87	-3.6	2.59	0.32	1.15	0.83	10.65	0.18	0.15
0.0200	14.71	0.30	0.30	-0.83	-4.9	-2.47	0.32	1.15	0.83	10.61	0.21	0.21
0.0233	14.67	0.34	0.40	-2.65	-5.5	-7.06	0.32	1.14	0.82	10.57	0.25	0.29
0.0261	14.63	0.39	0.50	-4.13	-5.3	-8.66	0.32	1.14	0.82	10.53	0.28	0.36
0.0286	14.59	0.42	0.60	-5.18	-4.2	-6.85	0.32	1.14	0.82	10.49	0.30	0.44
0.0308	14.55	0.45	0.70	-5.70	-2.4	-2.62	0.32	1.14	0.82	10.45	0.33	0.51
0.0330	14.51	0.49	0.80	-5.69	0.1	2.91	0.32	1.13	0.81	10.41	0.35	0.58
0.0350	14.47	0.51	0.90	-5.10	2.9	7.15	0.32	1.13	0.81	10.37	0.37	0.65
0.0369	14.43	0.54	1.00	-4.02	5.7	8.66	0.32	1.13	0.81	10.33	0.39	0.73
0.0387	14.39	0.57	1.10	-2.54	8.2	6.85	0.32	1.12	0.80	10.29	0.41	0.80
0.0404	14.35	0.59	1.20	-0.84	10.0	2.49	0.32	1.12	0.80	10.25	0.43	0.87
0.0420	14.32	0.62	1.30	0.91	10.9	-2.69	0.32	1.12	0.80	10.21	0.44	0.94
0.0436	14.28	0.64	1.40	2.63	10.8	-7.02	0.32	1.11	0.79	10.17	0.46	1.01
0.0451	14.24	0.66	1.50	4.05	9.5	-8.66	0.32	1.11	0.79	10.14	0.47	1.08
0.0466	14.20	0.68	1.60	5.13	7.2	-7.05	0.32	1.11	0.79	10.10	0.49	1.15
0.0481	14.16	0.70	1.70	5.71	3.8	-2.56	0.32	1.10	0.78	10.06	0.51	1.23
0.0495	14.12	0.72	1.80	5.69	-0.1	2.78	0.32	1.10	0.78	10.02	0.52	1.30
0.0509	14.08	0.74	1.90	5.10	-4.2	7.15	0.32	1.10	0.78	9.98	0.53	1.37
0.0522	14.04	0.76	2.00	4.05	-8.1	8.66	0.32	1.10	0.78	9.94	0.55	1.44
0.0535	14.00	0.78	2.10	2.59	-11.3	6.94	0.32	1.09	0.77	9.90	0.56	1.51
0.0547	13.96	0.80	2.20	0.96	-13.5	2.85	0.32	1.09	0.77	9.86	0.57	1.58
0.0560	13.92	0.81	2.30	-0.92	-14.5	-2.73	0.32	1.09	0.77	9.82	0.58	1.66
0.0572	13.88	0.83	2.40	-2.61	-14.1	-7.00	0.32	1.08	0.76	9.78	0.60	1.73
0.0584	13.84	0.85	2.50	-4.08	-12.2	-8.66	0.32	1.08	0.76	9.74	0.61	1.80
0.0596	13.80	0.86	2.60	-5.16	-9.0	-6.91	0.32	1.08	0.76	9.70	0.62	1.87
0.0607	13.76	0.88	2.70	-5.70	-4.8	-2.74	0.32	1.07	0.75	9.66	0.63	1.94
0.0618	13.73	0.89	2.80	-5.71	-0.1	2.48	0.32	1.07	0.75	9.62	0.64	2.01
0.0629	13.69	0.91	2.90	-5.18	4.8	6.85	0.32	1.07	0.75	9.58	0.65	2.08
0.0640	13.65	0.92	3.00	-4.13	9.5	8.66	0.32	1.06	0.74	9.54	0.66	2.16
0.0651	13.61	0.94	3.10	-2.64	13.5	7.05	0.32	1.06	0.74	9.50	0.67	2.23
0.0662	13.57	0.95	3.20	-0.86	16.2	2.54	0.32	1.06	0.74	9.46	0.68	2.30
0.0672	13.53	0.97	3.30	0.88	17.3	-2.60	0.32	1.06	0.74	9.43	0.69	2.37
0.0682	13.49	0.98	3.40	2.55	16.8	-6.88	0.32	1.05	0.73	9.39	0.70	2.44
0.0693	13.45	1.00	3.50	4.14	14.4	-8.66	0.32	1.05	0.73	9.34	0.71	2.52

Table A.2 : (contd.) Movement and Magnetization Characteristics of The Integrated Type Designed Generator

Time	Stator			Flux $\times 10^{-5}$	EMF	Force(N)				Rotor		
	Acc.	Spd.	Pos.							Acc.	Spd.	Pos.
t (s)	a_s (m/s^2)	v_s (m/s)	X_s (cm)	Φ (Weber)	V	F_{my}	$\lvert\mu \times F_{my}\rvert$	F_r	F_n	a_r (m/s^2)	v_r (m/s)	X_r (cm)
0.0703	13.41	1.01	3.60	5.18	10.4	-6.85	0.32	1.05	0.73	9.30	0.72	2.59
0.0712	13.37	1.02	3.70	5.69	5.6	-2.87	0.32	1.04	0.72	9.27	0.73	2.66
0.0722	13.33	1.03	3.80	5.70	0.1	2.62	0.32	1.04	0.72	9.23	0.74	2.73
0.0732	13.29	1.05	3.90	5.12	-5.9	7.10	0.32	1.04	0.72	9.19	0.75	2.80
0.0741	13.25	1.06	4.00	4.11	-11.2	8.66	0.32	1.03	0.71	9.15	0.76	2.87
0.0751	13.21	1.07	4.10	2.55	-15.6	6.86	0.32	1.03	0.71	9.11	0.76	2.95
0.0760	13.17	1.08	4.20	0.87	-18.6	2.59	0.32	1.03	0.71	9.07	0.77	3.02
0.0769	13.13	1.10	4.30	-0.90	-19.7	-2.66	0.32	1.02	0.70	9.03	0.78	3.09
0.0778	13.09	1.11	4.40	-2.60	-18.9	-6.97	0.32	1.02	0.70	8.99	0.79	3.16
0.0787	13.05	1.12	4.50	-4.07	-16.3	-8.66	0.32	1.02	0.70	8.95	0.80	3.23
0.0796	13.01	1.13	4.60	-5.15	-12.0	-6.99	0.32	1.02	0.70	8.91	0.81	3.30
0.0805	12.97	1.14	4.70	-5.71	-6.2	-2.52	0.32	1.01	0.69	8.87	0.81	3.37
0.0814	12.93	1.15	4.80	-5.70	0.1	2.71	0.32	1.01	0.69	8.83	0.82	3.44
0.0822	12.90	1.17	4.90	-5.15	6.5	6.98	0.32	1.01	0.69	8.79	0.83	3.51
0.0831	12.86	1.18	5.00	-4.10	12.4	8.66	0.32	1.00	0.68	8.75	0.84	3.58
0.0839	12.82	1.19	5.10	-2.63	17.2	7.03	0.32	1.00	0.68	8.71	0.84	3.66
0.0848	12.78	1.20	5.20	-0.89	20.5	2.65	0.32	1.00	0.68	8.67	0.85	3.73
0.0856	12.74	1.21	5.30	0.95	21.7	-2.82	0.32	0.99	0.67	8.63	0.86	3.80
0.0864	12.70	1.22	5.40	2.62	20.8	-7.00	0.32	0.99	0.67	8.60	0.86	3.87
0.0872	12.66	1.23	5.50	4.05	17.9	-8.66	0.32	0.99	0.67	8.56	0.87	3.94
0.0880	12.62	1.24	5.60	5.11	13.3	-7.11	0.32	0.98	0.66	8.52	0.88	4.01
0.0888	12.58	1.25	5.70	5.69	7.2	-2.87	0.32	0.98	0.66	8.48	0.89	4.08
0.0896	12.54	1.26	5.80	5.71	0.3	2.50	0.32	0.98	0.66	8.44	0.89	4.15
0.0904	12.50	1.27	5.90	5.16	-6.9	6.93	0.32	0.98	0.66	8.40	0.90	4.22
0.0912	12.46	1.28	6.00	4.08	-13.4	8.66	0.32	0.97	0.65	8.36	0.91	4.29
0.0920	12.42	1.29	6.10	2.58	-18.8	6.93	0.32	0.97	0.65	8.32	0.91	4.37
0.0928	12.38	1.30	6.20	0.91	-22.2	2.70	0.32	0.97	0.65	8.28	0.92	4.43
0.0935	12.34	1.31	6.30	-0.85	-23.5	-2.53	0.32	0.96	0.64	8.24	0.92	4.50
0.0943	12.30	1.32	6.40	-2.55	-22.6	-6.87	0.32	0.96	0.64	8.20	0.93	4.57
0.0951	12.26	1.33	6.50	-4.10	-19.4	-8.66	0.32	0.96	0.64	8.16	0.94	4.65
0.0958	12.22	1.34	6.60	-5.15	-14.0	-6.96	0.32	0.95	0.63	8.12	0.94	4.72
0.0966	12.18	1.35	6.70	-5.70	-7.4	-2.58	0.32	0.95	0.63	8.08	0.95	4.79
0.0973	12.14	1.35	6.80	-5.69	0.2	2.84	0.32	0.95	0.63	8.04	0.96	4.86
0.0980	12.11	1.36	6.90	-5.15	7.6	6.95	0.32	0.94	0.62	8.00	0.96	4.93
0.0988	12.07	1.37	7.00	-4.07	14.5	8.66	0.32	0.94	0.62	7.96	0.97	5.00
0.0995	12.03	1.38	7.10	-2.55	20.2	6.87	0.32	0.94	0.62	7.92	0.97	5.07
0.1002	11.99	1.39	7.20	-0.88	23.9	2.62	0.32	0.93	0.61	7.88	0.98	5.14
0.1009	11.95	1.40	7.30	0.88	25.2	-2.61	0.32	0.93	0.61	7.85	0.98	5.21
0.1016	11.91	1.41	7.40	2.57	24.1	-6.90	0.32	0.93	0.61	7.81	0.99	5.28

Table A.2 : (contd.) Movement and Magnetization Characteristics of The Integrated Type Designed Generator

Time	Stator			Flux $\times 10^{-5}$	EMF	Force(N)				Rotor		
	Acc.	Spd.	Pos.							Acc.	Spd.	Pos.
t (s)	a_s (m/s^2)	v_s (m/s)	X_s (cm)	Φ (Weber)	V	F_{my}	$\lvert\mu \times F_{my}\rvert$	F_r	F_n	a_r (m/s^2)	v_r (m/s)	X_r (cm)
0.1023	11.87	1.41	7.50	4.02	20.8	-8.66	0.32	0.93	0.61	7.77	0.99	5.35
0.1031	11.83	1.42	7.60	5.16	15.1	-6.94	0.32	0.92	0.60	7.73	1.00	5.42
0.1038	11.79	1.43	7.70	5.70	7.8	-2.58	0.32	0.92	0.60	7.69	1.01	5.49
0.1045	11.75	1.44	7.80	5.69	-0.2	2.80	0.32	0.92	0.60	7.65	1.01	5.56
0.1052	11.71	1.45	7.90	5.11	-8.3	7.12	0.32	0.91	0.59	7.61	1.02	5.64
0.1058	11.67	1.46	8.00	4.11	-15.5	8.66	0.32	0.91	0.59	7.57	1.02	5.70
0.1065	11.63	1.46	8.10	2.62	-21.3	7.00	0.32	0.91	0.59	7.53	1.03	5.77
0.1072	11.59	1.47	8.20	0.85	-25.2	2.53	0.32	0.90	0.58	7.49	1.03	5.85
0.1079	11.55	1.48	8.30	-0.88	-26.7	-2.61	0.32	0.90	0.58	7.45	1.04	5.91
0.1085	11.52	1.49	8.40	-2.54	-25.6	-6.85	0.32	0.90	0.58	7.41	1.04	5.98
0.1092	11.47	1.50	8.50	-4.07	-21.9	-8.66	0.32	0.89	0.57	7.37	1.05	6.05
0.1099	11.43	1.50	8.60	-5.18	-15.8	-6.86	0.32	0.89	0.57	7.33	1.05	6.13
0.1106	11.39	1.51	8.70	-5.71	-8.1	-2.55	0.32	0.89	0.57	7.29	1.06	6.20
0.1112	11.36	1.52	8.80	-5.70	0.1	2.72	0.32	0.89	0.57	7.25	1.06	6.26
0.1119	11.32	1.53	8.90	-5.14	8.5	7.00	0.32	0.88	0.56	7.21	1.07	6.33
0.1125	11.28	1.53	9.00	-4.09	16.2	8.66	0.32	0.88	0.56	7.17	1.07	6.40
0.1132	11.24	1.54	9.10	-2.63	22.4	7.04	0.32	0.88	0.56	7.13	1.08	6.47
0.1138	11.20	1.55	9.20	-0.91	26.5	2.71	0.32	0.87	0.55	7.10	1.08	6.54
0.1145	11.16	1.55	9.30	0.91	28.0	-2.69	0.32	0.87	0.55	7.06	1.09	6.61
0.1151	11.12	1.56	9.40	2.64	26.7	-7.05	0.32	0.87	0.55	7.02	1.09	6.68
0.1158	11.08	1.57	9.50	4.12	22.7	-8.66	0.32	0.86	0.54	6.98	1.09	6.76
0.1164	11.04	1.58	9.60	5.16	16.5	-6.93	0.32	0.86	0.54	6.94	1.10	6.82
0.1170	11.00	1.58	9.70	5.70	8.6	-2.58	0.32	0.86	0.54	6.90	1.10	6.89
0.1176	10.96	1.59	9.80	5.69	-0.2	2.77	0.32	0.85	0.53	6.86	1.11	6.96
0.1183	10.92	1.60	9.90	5.12	-9.1	7.07	0.32	0.85	0.53	6.82	1.11	7.03
0.1189	10.88	1.60	10.00	4.04	-17.2	8.66	0.32	0.85	0.53	6.78	1.12	7.10
0.1195	10.84	1.61	10.10	2.55	-23.7	6.87	0.32	0.85	0.53	6.74	1.12	7.17
0.1201	10.80	1.62	10.20	0.86	-27.8	2.54	0.32	0.84	0.52	6.70	1.12	7.24
0.1208	10.76	1.62	10.30	-0.93	-29.3	-2.75	0.32	0.84	0.52	6.66	1.13	7.31
0.1214	10.72	1.63	10.40	-2.63	-27.9	-7.03	0.32	0.84	0.52	6.62	1.13	7.38
0.1220	10.68	1.64	10.50	-4.08	-23.8	-8.66	0.32	0.83	0.51	6.58	1.14	7.45
0.1226	10.64	1.64	10.60	-5.14	-17.4	-6.99	0.32	0.83	0.51	6.54	1.14	7.52
0.1232	10.60	1.65	10.70	-5.70	-9.1	-2.63	0.32	0.83	0.51	6.50	1.14	7.59
0.1238	10.57	1.66	10.80	-5.69	0.1	2.76	0.32	0.82	0.50	6.46	1.15	7.66
0.1244	10.53	1.66	10.90	-5.12	9.5	7.10	0.32	0.82	0.50	6.42	1.15	7.73
0.1250	10.49	1.67	11.00	-4.02	18.0	8.66	0.32	0.82	0.50	6.38	1.16	7.80
0.1256	10.45	1.68	11.10	-2.54	24.7	6.85	0.32	0.81	0.49	6.34	1.16	7.87
0.1262	10.41	1.68	11.20	-0.83	28.9	2.48	0.32	0.81	0.49	6.30	1.16	7.94
0.1268	10.37	1.69	11.30	0.93	30.4	-2.75	0.32	0.81	0.49	6.27	1.17	8.00

CURRICULUM VITA

Candidate's full name: Fatih Gürdal

Place and date of birth: Isparta 01-01-1983

Permanent Address: Melekhatun Mah. Başbakkal Meydanı Sok. 11/13

Fatih/İstanbul

Universities and Colleges attended: Middle East Technical University Electrical&Electronics Engineering Department (2001-2006)

Isparta Süleyman Demirel Fen Lisesi (1998-2001)